Literature Overview

Battlefield Damage Assessment in European Conflict Zones Using Multimodal (RGB + SAR) Satellite Images and Deep Neural Networks

Figure 1: Satellite View of Destruction in Ukraine. Source: Maxar ("Open Data Program," n.d.)

Studiengang MSc Geoinformationswissenschaften und Systeme,

Paris Lodron Universität Salzburg – UNIGIS

Thun, 30.08.2025, Marco Heinzen u107130

An Overview of Studies Utilizing Machine Learning (ML) Techniques for Post-Disaster or Conflict-Zone Urban Damage Assessment Using Remote Sensing.

Notes on Classification:

This document is classified as public.

Notes on Formatting:

For scripts and CLI inputs, the following highlighting is used:

```
#HIER             IST             EIN             CODE             BEISPIEL
CODE
```

Contents

1 Literature Overview

1.1 Abstract

Armed conflicts in urban environments generate complex patterns of structural damage that demand rapid, scalable, and accurate assessment methods. This study synthesizes foundations of remote sensing and machine learning to establish a framework for battlefield damage assessment of urban structures. The work integrates active and passive sensing modalities, including SAR and optical systems, with advanced ML architectures such as U-Nets, Siamese networks, generative adversarial models, and ensembles. Open datasets and satellite constellations provide global coverage, while UAV-based photogrammetry enables fine-scale validation.

The findings highlight three consistent themes: (1) multimodal fusion of SAR and optical data significantly enhances detection reliability under adverse conditions; (2) imbalance in benchmark datasets continues to bias model performance, particularly in intermediate damage classes; and (3) models trained on post-disaster contexts exhibit reduced transferability to conflict settings without domain adaptation. European building typologies and operational constraints, such as cloud cover, SAR jamming, and access restrictions, further shape applicability.

This overview concludes that robust battlefield damage assessment requires integrated RS–ML pipelines that combine event-held-out training, explainable inference, and multimodal fusion. These approaches enable more credible and operationally relevant assessments, supporting humanitarian relief, situational awareness, and defense planning in conflict-affected urban areas.

1.2 Introduction

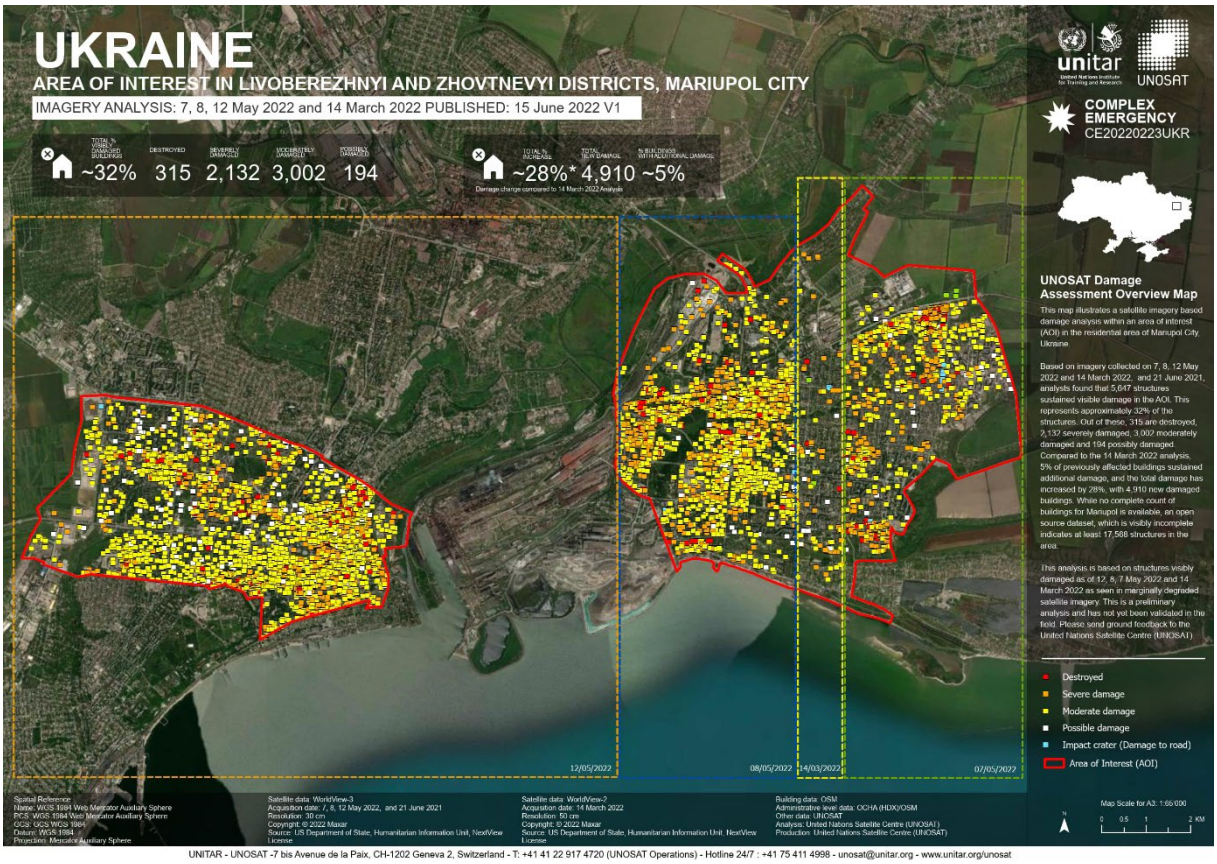

Figure 2: Map illustrating a satellite imagery based damage analysis within an area of interest (AOI) in the residential area of Mariupol City, Ukraine. ("UNOSAT" 2022)

Battlefield Damage Assessment (BDA) of urban structures lies at the intersection of Geospatial Intelligence (GEOINT) and remote sensing, where the interpretation of imagery supports decision-making in conflict zones. The historical trajectory of GEOINT shows how mapping, remote sensing, and geoinformatics converged into an intelligence discipline focused on actionable situational awareness (Clark 2020). Foundational texts such as Introduction to Remote Sensing (James B. Campbell and Randolph H. Wynne 2011), Remote Sensing: Digital Image Analysis (Richards 2022), and Introduction to Microwave Remote Sensing (Woodhouse 2017) provide the remote sensing and microwave principles on which GEOINT builds (Clark 2020; O'Connor 2024).

Armed conflicts in urban areas cause widespread destruction of civilian and military infrastructure (*Armed Conflict in the East of Ukraine* 2019; Garzón and Valánszki 2020). The consequences extend beyond the immediate battlefield, shaping humanitarian crises, civil protection, economic decision-making, and strategic military planning (Aimaiti et al. 2022; *Armed Conflict in the East of Ukraine* 2019). Urban damage assessment in post-disaster and conflict zones has therefore gained urgency due to the scale, complexity, and geopolitical

significance of recent crises (Plank 2014; Endo et al. 2018). Accurate and timely information on the state of urban structures is vital not only for humanitarian relief and reconstruction but also for situational awareness and battlefield decision-making (Benson and Ecker 2020).

In European conflict theaters such as the Second World War, the Balkans, and, more recently, Ukraine, large-scale destruction of housing and infrastructure has forced millions to flee, creating humanitarian emergencies across the (*Armed Conflict in the East of Ukraine* 2019; Garzón and Valánszki 2020). Rapid and reliable evaluation of structural damage is thus a critical capability for both defense and civil protection organizations (Clark 2020; Butenko and Petrychenko 2023; Shelestov et al. 2023). International actors, including the United Nations (UN), the European Union (EU), and the International Committee of the Red Cross (ICRC), rely on objective situational awareness to estimate displacement, coordinate aid, and prioritize reconstruction ("UN" 2025; "ICRC" 2025; "European Union" 2025; "UNOSAT," n.d.; "Ukraine Conflict Monitor ACLED" 2025). For Switzerland, a country committed to neutrality, humanitarian aid, and diplomacy, and as the host of major international organizations, remote sensing provides a means to support neutral yet informed responses to crises.

Remote sensing has long enabled the monitoring of large areas without physical access: from balloons in the First World War and aerial reconnaissance in the Second, to Cold War military satellites and the launch of Landsat-1 in 1972 (James B. Campbell and Randolph H. Wynne 2011). Since then, Earth observation has evolved into a multidisciplinary field encompassing optical, thermal, multispectral, hyperspectral, and radar sensors. Of particular importance are synthetic aperture radar (SAR) systems, which operate independently of daylight and can penetrate clouds, enabling all-weather, day-and-night monitoring (Flores et al. 2019). In parallel, artificial intelligence (AI) and machine learning (ML) have transformed automated image interpretation. Early pixel-based classifiers have been supplanted by object-based approaches and deep learning methods such as convolutional neural networks (CNNs), encoder–decoder architectures like U-Net, and more recent generative and graph-based models (Ronneberger et al. 2015; Chen et al. 2022).

The objective of this literature overview is to consolidate the state of knowledge on remote sensing and AI methods for battlefield damage assessment of urban structures. It situates existing work from the disaster and conflict monitoring domains, analyzes available sensors and datasets, and evaluates machine learning approaches for structural damage detection. By integrating insights from both civilian disaster management and defense-oriented studies, the review highlights the dual-use nature of these methods and establishes a scientific foundation for their application to conflict-related damage assessment in European theaters of operation.

From a civil protection perspective, rapid damage assessment after natural disasters is essential for directing emergency services and estimating losses. UAV-based mapping, such as the surveys conducted by Swisstopo after the landslide in Blatten (Lötschental), demonstrates how local authorities can quickly identify destroyed buildings and allocate resources efficiently. Such methods are also valuable for insurance companies in cost estimation. Although this thesis primarily addresses conflict-related applications, the methodological parallels with

natural disaster management underline the dual-use value of remote sensing and AI ("Swisstopo Fliegt Rapid-Mapping-Einsatz Bei Blatten" 2025).

From a military and intelligence perspective, damage assessment provides independent, global insight into conflict progression. Satellite imagery—optical, multispectral, hyperspectral, or radar-based—enables analysts to identify destroyed urban areas, assess whether roads and bridges remain functional, and evaluate how infrastructure damage constrains both civilian and military mobility. For friendly forces, such information supports tactical planning, emergency response, urban operations, and post-conflict stabilization. For adversaries, assessments reveal whether occupied structures remain usable or whether destroyed supply routes impede maneuverability. Beyond tactical applications, such intelligence supports strategic evaluations of conflict progression, enabling states to anticipate humanitarian flows, economic disruption, and security dynamics (Clark 2020; O'Connor 2024).

The foundation of automated assessment workflows lies in the acquisition and comparison of pre- and post-event imagery. Very high resolution (VHR) optical satellites provide detailed coverage, while radar platforms ensure all-weather monitoring. SAR interferometry (InSAR) adds depth by capturing subtle deformations invisible to optical sensors (Richards 2022). Multispectral and hyperspectral imagery support land-use classification and enable the targeting of analysis to defined areas of interest, reducing computational requirements (Jensen 2016; James B. Campbell and Randolph H. Wynne 2011; Richards 2022). Benchmark datasets such as xBD (Gupta et al. 2019) and SpaceNet (Etten et al. 2018) are widely used to train and validate models, but conflict-specific datasets are increasingly recognized as essential for transferability across urban morphologies (Benson and Ecker 2020; Scher and Van Den Hoek 2025). Robust preprocessing - including image co-registration, domain shift correction, indexing, and land-use classification - ensures comparability across timeframes and sensors (X. X. Zhu et al. 2017; Meyer 2019). Dimensionality reduction methods (e.g., PCA, autoencoders) and filtering approaches further reduce noise and extract meaningful features (Green et al. 1998; I. T. Jolliffe 2002; Richards 2022; Hinton and Salakhutdinov 2006).

Recent advances in deep learning architectures have expanded the possibilities of urban damage detection. CNNs (Su et al. 2020), U-Nets (Wu et al. 2021), Siamese networks (Khvedchenya and Gabruseva 2021), Swin Transformers (Cui et al. 2023), and attention-based frameworks (Hao et al. 2021; Shen et al. 2022) enable precise footprint extraction and multi-class damage classification (Wang et al. 2024; Taiwo H. Agbaje et al. 2024). Transfer learning (Zheng et al. 2024; Liu et al. 2020b; Bouchard et al. 2022), GAN-based augmentation (Su et al. 2020), and multimodal fusion (optical + SAR) improve robustness across regions and disaster types (Endo et al. 2018; Adriano et al. 2021), while hyperparameter optimization enhances generalization (Goodfellow et al. 2016). Outputs are increasingly delivered as GIS-compatible layers—polygon segmentations and ordinal damage scales—that integrate into situational awareness platforms such as QGIS, GeoServer (Calantropio et al. 2021), or web dashboards ("UNOSAT," n.d.; Chawanji et al. 2022). Emerging developments include 3D structural modeling (Fernández Galarreta et al. 2015), near-real-time UAV analytics (Liu et al. 2020b;

Calantropio et al. 2021; Alphonse et al. 2023; Kerle et al. 2020; Hewawiththi et al. 2024), and cloud-integrated ML pipelines (Dietrich et al. 2025). Yet, these methods highlight the problem of transferability: most models are trained on globally diverse datasets such as xBD, which suffer from class imbalance (Gupta et al. 2019; Su et al. 2020; Benson and Ecker 2020) and underrepresentation of European building typologies (Al Shafian et al. 2025; Wang et al. 2022).

ML models have already achieved strong results in natural disaster contexts, including earthquake (Cui et al. 2023; Xia et al. 2023; Voigt et al. 2011; ZHAO Jinling 2024; Qing et al. 2022; Ji et al. 2018; Rao et al. 2023), hurricane (Cheng et al. 2021; Li et al. 2018b; Cao and Choe 2024; 2020; Li et al. 2018a; 2024) and wildfire damage mapping (Kang et al. 2025). Since 2018, emerging studies have begun to address conflict-related damage assessment directly, applying RS and ML approaches to Syria (Braun 2018; Lubin and Saleem 2019; Joy-Fares, n.d.; Casana and Laugier 2017; Lubin and Saleem 2019), Iraq (Boloorani et al. 2021), and Ukraine (Dietrich et al. 2025; Scher and Van Den Hoek 2025; Butenko and Petrychenko 2023; Aimaiti et al. 2022; Kholoshyn et al. 2023), often using Sentinel-1/2 and WorldView imagery. UNOSAT products are frequently employed as reference data for validation (Chawanji et al. 2022; “UNOSAT,” n.d.). However, this literature remains limited compared to civilian disaster studies. Much of the methodological foundation stems from natural-disaster assessments. By contrast, battlefield monitoring faces contested access, deliberate denial and deception measures, and sometimes active jamming of optical and radar systems (O’Connor 2024; Clark 2020).

Major challenges remain. Data scarcity and limited labeled datasets - particularly in European conflict zones - restrict model generalization. Domain adaptation is a persistent bottleneck, as models trained on one region or conflict often underperform in new geographies (Benson and Ecker 2020). Urban heterogeneity, partial destruction, and the lack of annotated datasets covering non-building infrastructure (roads, bridges, utilities) further complicate operational deployment. In conclusion, this literature overview underscores the potential of combining remote sensing and AI for rapid, accurate, and scalable battlefield damage assessment. By integrating humanitarian, civil protection, and defense intelligence perspectives, and by systematically reviewing sensors, datasets, and algorithms, the study bridges the gap between academic innovation and operational readiness in conflict-sensitive environments.

1.3 Data Acquisition

Satellite remote sensing data acquisition underpins both post-disaster assessment and battlefield damage assessment first steps be it by automated ML pipelines or specialists. The operational data regime differs primarily in emphasis - latency, tasking priority, and dissemination constraints - rather than in the fundamental sources available to analysts (Chawanji et al. 2022; “UNOSAT,” n.d.; “UNOSAT,” n.d.; “Battle Damage Assessment - an Overview | ScienceDirect Topics,” n.d.; Andress 2014). In European civil-protection contexts, rapid mapping routinely exploits pre/post image pairs together with sanctioned airborne acquisitions; Switzerland has institutionalized such rapid campaigns, with swisstopo delivering obliques and quick orthophotos within hours to days, exemplified by the May 2025 Rapid-Mapping mission above Blatten in the Lötschental (“Swisstopo Fliegt Rapid-Mapping-Einsatz Bei Blatten” 2025). In parallel, authoritative satellite-derived analysis from Copernicus EMS Rapid Mapping and UNOSAT can be activated for large natural disasters and selected conflicts of international concern, providing standardized impact delineation and graded damage products on a 24/7 basis and following well-defined activation, production, and dissemination pipelines (“UNOSAT,” n.d.; Chawanji et al. 2022). Commercial constellations complement these public services: Maxar’s Open Data Program releases pre/post WorldView-class imagery openly for major crises to support humanitarian mapping (“Unlocking The Power Of Space For Disaster Mitigation And Humanitarian…,” n.d.), while WorldView Tasking offers priority collections for emergency response with high daily capacity (“Open Data Program,” n.d.). For downstream ML analysis, the canonical pre/post sources include ESA’s Sentinel-1 (C-band SAR) and Sentinel-2 (multispectral optical) constellations—valuable for global coverage and open access—augmented, where available, by very-high-resolution commercial sensors such as the WorldView series for fine-scale damage grading (“Rapid Access Program | Commercial Imaging Satellites,” n.d.; Berger et al. 2012; Torres et al. 2012; Drusch et al. 2012; Torres et al. 2012).

In armed conflict, both pre- and post-event satellite imagery are generally available to state and commercial actors; what shifts materially are access priority, tasking latency, and permissions for public release (Andress 2014). The datasets are sometimes complemented by very-high-resolution (VHR) commercial sensors such as Maxar/DigitalGlobe’s WorldView and GeoEye platforms and Airbus’ Pléiades programme, which offer finer detail but are restricted by licensing and cost (Wulder et al. 2019). Commercial very-high-resolution constellations advertise sub-daily revisit and hour-scale emergency tasking/delivery pathways—service levels that vary by provider and tier across Pléiades Neo, WorldView/Legion, and SkySat (“Rapid Access Program | Commercial Imaging Satellites,” n.d.; “SkySat Full Archive and New Tasking - Earth Online,” n.d.; “Defence | Airbus” 2024; “Pléiades Neo Full Archive and Tasking - Earth Online,” n.d.). Nevertheless, optical imaging remains constrained by clouds, haze, smoke, and illumination geometry, whereas SAR mitigates weather and diurnal limitations but introduces foreshortening, layover/shadow, and coherence decorrelation that require specialist processing (Meyer 2019; Richards 2022). Consequently, operational agencies exploit pre/post pairs when available and default to SAR-led or fused SAR-optical solutions when

optical collections are degraded or embargoed, a pattern documented in reviews and recent Ukraine casework (Plank 2014; Adriano et al. 2021; Aimaiti et al. 2022). The main point is not that only post-event imagery exists in war, but that latency, atmospheric obscuration, emission-control and classification constraints make sensor choice and temporal pairing contingent rather than guaranteed, especially for public-release products (Andress 2014; Richards 2022; Meyer 2019). A recurring theme in the literature is the increasing reliance on open-access satellite missions, particularly ESA's Sentinel-1 synthetic aperture radar (SAR) (Plank 2014; Dietrich et al. 2025; Aimaiti et al. 2022) and Sentinel-2 multispectral optical constellation (Aimaiti et al. 2022; El Mendili et al. 2020), which provide systematic, free, and global coverage (Berger et al. 2012). The choice of sensor is conditioned by trade-offs between spatial resolution, spectral richness, and revisit frequency, with Sentinel missions optimized for systematic monitoring and VHR commercial constellations tailored for fine-scale event mapping (Richards 2022; Jensen 2016).

The acquisition of cloud-free optical, very-high-resolution, multispectral, or hyperspectral imagery is constrained by revisit schedules, atmospheric conditions such as cloud cover, and high procurement costs (Berger et al. 2012; Wulder et al. 2019; Richards 2022; James B. Campbell and Randolph H. Wynne 2011). Emerging hyperspectral missions such as PRISMA, EnMAP, and the forthcoming CHIME and NASA SBG will further enable material-level discrimination of rubble, roofing, and debris through narrow-band imaging spectroscopy (Guanter et al. 2015; Loizzo et al. 2018; Thenkabail et al. 2023).

Public benchmark datasets such as xBD (Gupta et al. 2019; Su et al. 2020) and SpaceNet (Etten et al. 2018) have become foundational for developing and evaluating AI models, since they combine broad geographic and temporal coverage with detailed building footprints and multi-class damage annotations. Despite these advances, important gaps remain. Precompiled benchmark datasets often have limited representation of European or Western urban morphologies, constraining transferability of trained models across regions (Benson and Ecker 2020; Al Shafian et al. 2025).

Unmanned aerial vehicles (UAVs) have emerged as indispensable for localized validation and very-high-detail mapping, bridging the spatial and temporal gap where satellites cannot provide timely or sufficiently granular coverage (Liu et al. 2020b; Hewawiththi et al. 2024; Alphonse et al. 2023; Calantropio et al. 2021; Kerle et al. 2020). Humanitarian mapping programs, including Copernicus Emergency Management Service (EMS) (Chawanji et al. 2022) and UNOSAT ("UNOSAT," n.d.), provide critical reference datasets for calibration and validation, but these are typically limited to major international events and may lag in update frequency (Flores et al. 2019; Richards 2022). Finally, crowdsourced platforms such as OpenStreetMap ("BaseMap - GEOINT | OSM," n.d.), which provides community-validated building footprints (Heipke 2010; Herfort et al. 2021), and Tomnod, which facilitated large-scale disaster annotation campaigns (Ziemke 2012; Maxar 2019), contribute valuable data for crisis mapping. However, their accuracy and geographic completeness are uneven, requiring careful quality assessment before operational integration (Kerle et al. 2020).

Pre- and post-disaster remote sensing imagery acquisition forms the foundation of urban damage assessment in post-conflict and disaster scenarios. High-resolution satellite imagery, such as the 0.5 m WorldView-2 data used by (Xia et al. 2023), enables fine-grained structural damage detection at the pixel level, revealing collapse patterns and deformation unobservable in coarser datasets. Similarly, Rashidian et al. (2021) demonstrate the utility of 30 cm RGB imagery, which facilitates rapid- and accurate damage mapping (Rashidian et al. 2021). The xBD dataset by Gupta et al. (2019), constructed with annotated pre- and post-disaster imagery, provides a standardized benchmark for training machine learning models across various disaster types (Gupta et al. 2019; Su et al. 2020). UAVs offer ultra-high-resolution and flexible data collection alternatives, as highlighted by Cheng et al. (2021), who used drone imagery after Hurricane Dorian for FEMA-scale preliminary damage assessment, and by (Soulakellis et al. (2019), who combined UAVs, terrestrial laser scanning, and Structure-from-Motion (SfM) to build detailed 3D models of earthquake-affected areas in Lesvos (Cheng et al. 2021; Soulakellis et al. 2019). Broader approaches to damage detection include multi-temporal and single-temporal remote sensing (Gupta et al. 2024; Kholoshyn et al. 2023), with the latter gaining importance in conflict zones where pre-disaster imagery is unavailable. Multimodal sensor fusion, integrating optical and radar data (Selvakumaran et al. 2025), enhances assessment reliability in visually obstructed or dynamically evolving settings. Sentinel-1 SAR (Plank 2014) provides weather-independent, frequent imaging suitable for all-season monitoring, though interpretation in dense urban areas remains challenged by layover, foreshortening, and shadow effects that complicate damage extraction (Meyer 2019; Richards 2022), while Sentinel-2's multispectral bands support urban land cover mapping by capturing seasonal and spectral variations (El Mendili et al. 2020; Richards 2022; James B. Campbell and Randolph H. Wynne 2011). Structural change detection methods, including pixel-based differencing, object-oriented analysis, and mathematical morphology (Wu et al. 2021), are essential in dense urban environments where accurate damage mapping is challenged by misalignment, shadows, and spectral confusion.

The complete lists and tables of satellites, datasets, and repositories that underpin this study are provided in the appendix (see Appendix 3.2 *Data Sources*, including 3.2.1 *Table of Satellites*, 3.2.2 *Table of Datasets and Data Sources*, and 3.2.3 *List of Datasets and Data Repositories*).

1.4 Preprocessing

1.4.1 Image Preprocessing and Enhancement

Image preprocessing is a critical step in enabling accurate machine learning-based damage assessment of urban structures from remote sensing data, especially in conflict zones and disaster-hit regions. A major challenge in multi-temporal analysis is image misalignment, which can significantly impair pixel-level comparisons; thus, co-registration techniques are essential for ensuring spatial consistency across pre- and post-disaster imagery (Kim and Han 2021). For reproducible, scalable inference, multimodal stacks (e.g., Sentinel-1/2, VHR, hyperspectral) should be orthorectified, co-registered, and stored as aligned tensors with explicit band semantics and missing-data masks, then read as consistent slices during training and deployment. This data-cube style abstraction, widely used in modern EO platforms, ensures that segmentation and feature extractors ingest harmonised inputs and that SAR-specific preprocessing (speckle filtering, RTC) is preserved in provenance metadata (Richards, 2022, Remote Sensing Digital Image Analysis; Meyer, 2019, Spaceborne Synthetic Aperture Radar – Principles, Data Access, and Basic Processing Techniques). Seasonal variations, cloud cover, and visual distortions such as fog or lighting inconsistencies further complicate interpretation, necessitating robust preprocessing and enhancement techniques. Fundamental preprocessing steps include radiometric calibration, atmospheric correction to remove scattering and absorption effects, and geometric correction to ensure consistent georeferencing across scenes, all of which are prerequisites for reliable temporal analysis (Richards 2022; Jensen 2016). To this end, advanced models like the Swin Transformer with CBAM and multilevel feature fusion have shown improved performance under degraded imaging conditions (Cui et al. 2023). Addressing temporal domain shifts - caused by changes in season, environment, or structural layout - (Mueller et al. 2021) propose temporal label alignment strategies to maintain annotation consistency across different observation periods. Supporting real-time and large-scale processing needs, (Wang et al. 2024) introduces a slice-assisted super inference strategy that divides large satellite images into overlapping tiles to optimize GPU usage without sacrificing resolution, facilitating high-throughput model deployment in operational environments. Similarly Li et al (2018) utilize Simple Linear Iterative Clustering (SLIC) as a preprocessing step for building candidate segmentation, enhancing the input quality for downstream CNN-based damage classification (Li et al. 2018b). In hyperspectral and multispectral contexts, dimensionality reduction methods such as Principal Component Analysis (PCA) and autoencoders help suppress redundancy and noise while retaining discriminative spectral-spatial features, improving classifier performance (Bioucas-Dias et al. 2013; Hinton and Salakhutdinov 2006). These preprocessing approaches are especially valuable when integrated into UAV workflows, as seen in (Hewawiththi et al. 2024) , where onboard deep learning models on UAVs filter and transmit only task-relevant information (e.g., structural damage classes), significantly improving efficiency in bandwidth-constrained or hostile settings. (Bhardwaj et al. 2025) and (Novikov et al. 2018) further demonstrate how automated workflows, which include preprocessing, dataset creation, segmentation model

training, and adaptive fine-tuning, can compress post-disaster damage mapping timelines from weeks or months to just hours, dramatically improving emergency response capabilities. Together, these studies establish that robust preprocessing pipelines, capable of handling noise, resolution variability and temporal inconsistency, are foundational to the success of remote sensing-based machine learning systems in rapid, accurate, and scalable battlefield or post-disaster structural damage assessment. Classical preprocessing techniques, including gradient- and Laplacian-based edge detection, Gaussian smoothing, and morphological filtering, remain important for enhancing feature boundaries in noisy or degraded images, often serving as the bridge between raw data and deep learning pipelines (Gonzalez and Woods 2018; Richards 2022).

1.4.2 Landuse Classification and Indexing

For urban building segmentation and battlefield damage assessment, a consistent finding across the reviewed work is that land-use classification is best treated as an early preprocessing gate (Selvakumaran et al. 2025). Rather than analyzing full scenes, several studies first delineate urban fabric at medium or high resolution and then restrict training and inference to those polygons, which improves class balance and removes large swaths of non-informative pixels (vegetation, water, bare soil) (Meyer 2019; Plank 2014). The effectiveness of such pre-masking reflects fundamental sensor trade-offs: while optical systems offer rich spectral indices for urban delineation, they remain cloud- and illumination-dependent, whereas SAR provides robust all-weather backscatter signals but is affected by geometric distortions such as layover and foreshortening in dense city cores (Richards 2022; Jensen 2016). In practice, this urban pre-mask can be obtained by fusing global built-up layers with scene-specific classifiers; for example, Sentinel-2 time-series urban mapping has proven reliable at city scale and varying seasons (El Mendili et al. 2020) and object-based segmentation has long been shown to stabilize change analyses in dense built environments (Al-Khudhairy et al. 2005). This reflects the broader Object-Based Image Analysis (OBIA) paradigm, which groups pixels into meaningful objects based on spectral, spatial, and contextual cues, thereby improving classification accuracy and reducing noise in heterogeneous urban scenes (Blaschke 2010; Richards 2022). In dense urban areas, mixed pixels are common, where rooftops, vegetation, and roads overlap at sub-pixel scales. Spectral unmixing approaches can decompose these mixtures into fractional endmembers, improving land-use classification where simple indices are insufficient (Clark et al. 2003; Thenkabail et al. 2023). Within the broader SAR literature, this front-loading step is also consistent with operational guidance: focusing processing on urban AOIs is a practical way to reduce both computational load and false alarm rates in crisis mapping (Meyer 2019; Plank 2014).

For urban delineation by indices, the literature converges on a compact, well-understood set derived from multispectral data: NDVI to suppress vegetation, NDWI/MNDWI to remove water, and NDBI together with composite built-up indices (e.g., IBI) to enhance impervious surfaces (Bioucas-Dias et al. 2013; El Mendili et al. 2020). It is important to note that two

widely used indices share the acronym NDWI: the green–NIR formulation designed for water body detection (McFeeters 1996) and the NIR–SWIR variant targeting vegetation liquid water content (Gao 1996), with the former being standard in urban masking workflows. These indices are routinely combined with simple decision rules and morphological cleaning to produce robust urban masks that generalise across European morphologies, while keeping manual tuning minimal (El Mendili et al. 2020). For multispectral and hyperspectral data, dimensionality reduction techniques such as Principal Component Analysis (PCA) and autoencoders are widely applied to compress redundant information while retaining discriminative spectral features for urban land-use classification (Bioucas-Dias et al. 2013; Hinton and Salakhutdinov 2006). Such morphological preprocessing—erosion, dilation, and opening/closing—remains a core technique in computer vision and remote sensing, often serving as a bridge between raw index maps and more advanced machine learning segmentation (Gonzalez and Woods 2018). Where optical data are limited by clouds or revisit, Sentinel-1 SAR provides additional urban cues, VV/VH backscatter and their ratios (double-bounce in built structure) and, for SLC stacks, coherence as a stability prior, helping to confirm built-up areas and maintain continuity through adverse conditions (Meyer 2019; Plank 2014). These polarization channels capture distinct scattering mechanisms: VV is sensitive to surface roughness, VH highlights volume scatter from vegetation, and strong HH or VV responses combined with reduced cross-pol indicate double-bounce interactions typical of vertical walls adjacent to streets, a diagnostic feature of urban morphology (Meyer 2019; Richards 2022; Van Zyl and Kim 2011).

The urban-only masking is not a cosmetic step but a computational and learning lever: it reduces the number of tiles to process, suppresses obviously negative background, and accelerates both training and inference without sacrificing coverage of the target class. In operational contexts, similar constraints of the processing domain, either by Area of Interest (AOI) sectorization or by class-driven pre-masking, are recommended to meet timeliness requirements (Selvakumaran et al. 2025). Historically, such workflows often relied on support vector machines, random forests, and decision trees for land-use classification, and although deep learning now dominates, these methods remain relevant for lightweight or small-sample applications (James B. Campbell and Randolph H. Wynne 2011; Richards 2022).

Table of Spectral Indices can be found in the Appendix section under Chapter 3.3

1.4.3 Data Fusion, multimodal Datasets and Data Formats

In the last years, a progression from single-modality (optical-only or SAR-only) to multimodal fusion and where available to hyperspectral enrichment can be discerned. Optical imagery (RGB plus NIR/SWIR from Sentinel-2) provides the spectral leverage for urban pre-masking and building/roof segmentation using established indices NDVI (vegetation suppression), NDWI/MNDWI (water suppression), and NDBI/IBI (imperviousness). SAR contributes all-weather structural sensitivity, notably C-band VV/VH amplitude and VV/VH ratio (double-

bounce from façades/edges) and where multi-temporal SLCs exist, coherence as a stability prior over built surfaces (Meyer 2019; Plank 2014; El Mendili et al. 2020). Polarization channels encode different scattering mechanisms: co-pol responses (e.g., VV) emphasize surface and double-bounce returns from façade–ground interactions typical of street canyons, while cross-pol (e.g., VH) highlights volume scattering from trees and rough vegetation; these contrasts are routinely exploited to separate built-up fabric from vegetated context in urban SAR mapping (Van Zyl and Kim 2011; Meyer 2019; Richards 2022). Where hyperspectral is available (contiguous VNIR/SWIR), narrow-band absorptions and mixture analysis can further separate urban materials and debris, strengthening post-event contrasts (Bioucas-Dias et al. 2013). Beyond narrow-band absorptions, spectral unmixing helps resolve mixed urban pixels (roofing, rubble, vegetation) at sub-pixel scales, improving land-use masks and post-event contrasts where index-based approaches saturate (Clark et al. 2003; Thenkabail et al. 2023). Across studies, fusing these complementary signals at feature or decision level, consistently improves robustness for urban building segmentation and damage mapping (Benedetti et al. 2018; Adriano et al. 2021). From a modeling perspective, feature-level fusion (shared backbones over stacked bands) and decision-level fusion (ensembling per-modality experts) reflect complementary strategies: the former learns cross-modal interactions directly, while the latter increases robustness under missing-modality conditions—aligning with ensemble learning principles summarized in the ML literature (Zhou 2012; Adriano et al. 2021).

A recurring practical constraint is pre/post availability in the same modality and format: clouds and tasking gaps limit optical pairs, SAR pairs may differ in geometry, hyperspectral coverage is sparse. Most papers first perform orthorectification and precise co-registration across modalities plus radiometric terrain correction (RTC) for SAR - to form a pixel-aligned multimodal stack that reduces geometry-driven artefacts in dense urban fabric (Meyer 2019; Plank 2014). Operationally, SAR stacks benefit from speckle suppression and consistent acquisition geometry: coherence requires closely matched track and viewing geometry, while layover, foreshortening and shadow in dense city cores motivate RTC and careful masking prior to fusion, in line with standard SAR processing guidance (Meyer 2019; Richards 2022). When a modality is missing (such as no pre-event optical), several works adopt cross-modal fusion, exploiting SAR-only change cues or optical-only proxies and training models to operate with masked/imputed channels rather than discarding AOIs (Adriano et al. 2021; Selvakumaran et al. 2025). In this framing, fusion is simultaneously a performance enhancer (when all sources exist) and a resilience strategy (when some do not), while keeping a consistent downstream interface for segmentation and damage assessment.

To process such heterogeneous stacks at scale, several authors and platforms move to data-cube/tensor abstractions that align space–time–bands on a common grid. In practice, these abstractions are supported by mature platforms and frameworks: Google Earth Engine provides petabyte-scale catalogs (Sentinel-1/2, Landsat, MODIS) and array-based cloud execution for space–time analysis, while open data-cube frameworks (e.g., Open Data Cube/GeoCubes implementations) maintain harmonized x–y–time–band tensors for reproducible ingestion and modeling. Conceptually similar global tensor constructs (e.g.,

AlphaEarth-style 10 m matrices) standardize resampling to an analysis grid (e.g., 10 m for S1/S2 fusion or nested schemes when VHR is included), record band provenance (RGB, NIR/SWIR, SAR VV/VH, hyperspectral channels), and persist binary masks for missing data—thereby enabling consistent orthorectification/co-registration/RTC, urban pre-masking, and fusion-ready feature extraction in one store (Meyer 2019; Richards 2022). Conceptual precedents include Google's AlphaEarth notion, a 10 m global matrix/tensor for multi-source EO (Brown et al. 2025) and the GeoCubes approach (Pondi et al. 2024) both of which keep the dimensions (x, y, time, band) in a single addressable object for efficient model ingestion. In practice, modalities are resampled to a chosen analysis grid (e.g., 10 m for Sentinel-1/2 fusion or a nested scheme when VHR is included), band semantics are recorded (RGB, NIR/SWIR, SAR VV/VH, any hyperspectral channels) and binary masks capture missing data. This enables reproducible preprocessing (orthorectification/co-registration/RTC), urban pre-masking, and fusion-ready feature extraction in one multimodal store, while training and inference read consistent tensor slices (per AOI, timestamp, band set). As shown in fusion studies (Benedetti et al. 2018; Adriano et al. 2021), pixel-aligned multimodal stacks coupled with data-cube/tensor storage provide a practical foundation for scalable, operational multimodal damage assessment.

1.5 ML Models

See Appendix section 3.4 for a complete table of ML Models used in compiled papers.

1.5.1 Segmentation and Feature Extraction

Feature extraction and segmentation are the two pillars of machine-learning pipelines for damage assessment because they determine what information downstream classifiers can actually learn. Early workflows coupled pixel-based transforms - Principal Component Analysis (PCA) (I. T. Jolliffe 2002; Jolliffe and Cadima 2016) and texture transforms with Object-Based Image Analysis (OBIA) to stabilize maps in dense urban areas (Blaschke 2010; Blaschke et al. 2014); early building-scale examples used IKONOS with change detection and object-oriented segmentation (Al-Khudhairy et al. 2005). OBIA formalised a now-standard practice in remote sensing ML: group pixels into semantically coherent objects first (superpixels/segments), then classify those objects using spectral, textural and shape features; this reduces salt-and-pepper noise and improves change consistency in cluttered street grids (Blaschke 2010; Richards 2022).

Modern segmentation has largely shifted to convolutional encoder–decoder architectures that operate directly on pre-/post-event imagery. In very-high-resolution (VHR) optical and aerial data, U-Net remains the workhorse for VHR building/roof segmentation; skip connections preserve boundary detail while deep encoders capture neighborhood context (Ronneberger et al. 2015; Richards 2022). Common backbones include ResNet (He et al. 2016), DenseNet (Huang et al. 2017) and EfficientNet (Tan and Le 2019). Recent adaptations for damage mapping include selective-kernel and dual-branch Siamese U-Nets that decouple footprint localisation from per-building damage classification across four ordinal levels (Ahmadi et al. 2023; H. Xie et al. 2022). Change detection with bi-temporal inputs has converged on Siamese encoders with weight sharing to learn pre/post invariances and highlight true structural change, often augmented by attention modules to suppress illumination/seasonal effects. When pre/post pairs are available, Siamese encoders with shared weights (often with attention) typically outperform single-temporal baselines on LEVIR/WHU/xBD-style tasks (Daudt et al. 2018; Chen et al. 2022). Recent challenge work supports this trend (Khvedchenya and Gabruseva 2021). For operational settings where only post-event imagery is available (e.g., conflict theatre), single-temporal segmentation/classification remains essential; multi-modal/multi-temporal datasets demonstrate viable post-only baselines and robust fusion options (Adriano et al. 2021).

Where SAR is used—either standalone in adverse conditions or fused with optical—feature extraction must respect radar physics. Amplitude stacks provide all-weather/night structural cues, and, where SLCs exist, interferometric coherence adds a strong stability prior over built surfaces. Co-pol channels emphasize rough surface/double-bounce in urban dihedrals, while cross-pol highlights vegetation volume. However, SAR also introduces speckle and geometric distortions (layover, foreshortening, shadow) that complicate interpretation. To ensure trustworthy, pixel-aligned inputs, preprocessing is essential: co-registration (including with

optical), speckle suppression, and radiometric terrain correction (RTC) are standard prerequisites and operational best practice before learning over amplitude, coherence, or polarimetric features (Meyer 2019; Richards 2022; Small 2011; Plank 2014).

Hand-crafted features still matter at VHR: spectral indices (e.g., NDVI/NDWI/NDBI/IBI), grey-level co-occurrence matrix (GLCM) textures, edge cues (gradient/Laplacian; Canny; LoG), and shape descriptors are routinely combined with morphological cleaning to stabilise masks and sharpen boundaries before or alongside deep models (Marr and Hildreth 1980; Gonzalez and Woods 2018; Richards 2022). PCA/MNF reduce redundancy/noise (Green et al. 1998; I. T. Jolliffe 2002; Jolliffe and Cadima 2016); linear spectral unmixing supports fractional abundances (roofing/rubble/vegetation) (Adams et al. 1986; Bioucas-Dias et al. 2013); Classical edge/texture cues remain valuable adjuncts (Gonzalez and Woods 2018; Canny 1986; Marr and Hildreth 1980).

Model families in current practice can be grouped into four layers:

First, classical baselines: SVM (Cortes and Vapnik 1995), Random Forest (Breiman 2001), decision trees (Quinlan 1986)) remain strong light-weight baselines and pre-maskers (James B. Campbell and Randolph H. Wynne 2011; Richards 2022).

Second, CNN encoder–decoders (U-Net/SegNet/UNet++/DeepLab) perform semantic segmentation of buildings and damage regions from VHR optical or pansharpened inputs (Ronneberger et al. 2015; Badrinarayanan et al. 2017; Zhang et al. 2024; Zhou et al. 2018; He et al. 2016; Tan and Le 2019), with ResNet/DenseNet/EfficientNet encoders as backbones chosen to balance speed and accuracy (He et al. 2016; Huang et al. 2017; Tan and Le 2019).

Third, Siamese and attention-augmented networks specialise in bi-temporal change and ordinal damage classification, including designs that cascade footprint segmentation and damage grading to mitigate label noise between “minor” and “major” classes (Daudt et al. 2018; Chen et al. 2022; Ahmadi et al. 2023).

Fourth, fusion models combine optical/SAR - and where available hyperspectral - either at feature-level (stacked bands into a shared backbone) or decision-level (ensembling modality-specific experts). Both strategies improve robustness across conditions and mitigate missing-modality gaps (Adriano et al. 2021).

At operational scale segmentation pipelines must meet latency and compute constraints. Graph-based methods propagate sparse labels across building graphs and exposes subjective-logic uncertainty (vacuity/dissonance) for triage (Selvakumaran et al. 2025). Such approaches explicitly reduce computational cost on low-power laptops while preserving interpretability and offering principled confidence measures to guide field decisions.

Training at scale demands attention to data imbalance, domain shift (sensor/platform, season, viewing) and limited labels. Practical remedies include curriculum sampling and class-balanced losses; data augmentation with geometric/photometric transforms; and, where labelled data are scarce, class-balanced sampling and generative augmentation via cGAN/CycleGAN (Mirza and Osindero 2014; X. X. Zhu et al. 2017; Goodfellow et al. 2014; Antoniou et al. 2018); self- and contrastive pretraining (e.g., SimCLR, BYOL, MoCo) improves invariance and transfer (Chen et al. 2020; Grill et al. 2020; He et al. 2020).

In summary, contemporary segmentation and feature-extraction pipelines for battlefield and post-disaster assessment combine (i) robust pre-/post-alignment, SAR-aware preprocessing, and OBIA/indices to stabilise inputs; (ii) encoder–decoder networks for footprints and debris mapping, often in Siamese form for change and ordinal damage; (iii) fusion of optical/SAR (and hyperspectral where available) at feature or decision level; and (iv) uncertainty-aware or graph-based modules where compute is scarce. This layered design reflects the physics of the sensors (spectral vs scattering), the structure of urban scenes (façade–street double-bounce; mixed pixels), and the realities of time-critical operations, delivering rapid and scalable maps without sacrificing interpretability (Meyer 2019; Richards 2022; Selvakumaran et al. 2025).

1.5.2 Damage Assessment

The realities of data acquisition (Chapter 1.3) drive model preferences. When reliable pre/post pairs exist, two-stream change networks capitalize on explicit temporal contrast. When only a post-event image can be exploited rapidly or consistently disseminated, single-temporal segmentation/classification remains essential. In cloud-prone or smoke-obscured conditions, SAR-aware feature learning or optical-SAR fusion is not merely an option but a robustness requirement supported by decades of SAR damage-mapping research and by recent Ukraine casework (Richards 2022; Plank 2014; Aimaiti et al. 2022; O'Connor 2024).

1.5.2.1 From photo-interpretation to deep learning: the post-disaster lineage

Operational BDA predates deep nets, progressing from expert photointerpretation (Clark 2020; O'Connor 2024) and pixel based image analysis (PBIA) - pixel transforms (differencing, PCA, textures)- (Voigt et al. 2007; 2011; 2016; Richards 2022) to object-based image analysis (OBIA) for stability under shadows/occlusions (Blaschke 2010; Blaschke et al. 2014; Burnett and Blaschke 2003); building-scale IKONOS workflows foreshadowed today's object-centric pipelines (Al-Khudhairy et al. 2005). In subsequent deep-learning systems, OBIA principles and urban morphology cues - shape, compactness, and contrast - persist as auxiliary features and regularizers, linking classical segmentation logic with modern encoder–decoder models (Blaschke et al. 2014; Richards 2022).

With the availability of larger annotated corpora, fully convolutional encoder–decoder models displaced shallow learners for building extraction and debris delineation. xBD and the xView2 Challenge catalyzed benchmarking, but they were not singular prerequisites for neural damage mapping. Rather, they standardized a global, ordinal taxonomy and released large-scale

pre/post VHR pairs that accelerated reproducibility and transfer experiments alongside other datasets and institutional products (Gupta et al. 2019; Su et al. 2020; Etten et al. 2018; Adriano et al. 2021; Etten and Hogan 2021). U-Net derivatives became the workhorse due to their boundary-preserving skip connections and encoder flexibility; SegNet, UNet++, DeepLab families, and PSP-style decoders appear across disaster studies depending on data regime and compute budgets (Ronneberger et al. 2015; Zhou et al. 2018; Badrinarayanan et al. 2017; Zhao et al. 2024; Touzani and Granderson 2021; Chen et al. 2017). VHR imagery is not the only, nor even the most common, substrate: Sentinel-2 and moderate-resolution sources remain widely used for regional screening, with VHR reserved for confirmation and fine-grained grading (Jensen 2016; Richards 2022).

1.5.2.2 Disaster Damage Assessment

Disaster damage assessment with machine learning has consolidated around a small set of architectural families whose choices mirror data availability and operational constraints. Fully convolutional encoder–decoder models remain foundational: U-Net and successors such as UNet++ and SegNet provide boundary-preserving segmentation with flexible encoders, and numerous disaster studies report strong performance for footprint extraction and debris delineation on both very-high-resolution (e.g., WorldView-class) and Sentinel-2 imagery (Ronneberger et al. 2015; Zhou et al. 2018; Badrinarayanan et al. 2017). Siamese change-detection architectures fuse pre/post pairs with shared-weight encoders and mid-level feature fusion, outperforming single-image baselines when pairs are available and thereby suiting damage inference from bi-temporal inputs (Daudt et al. 2018; Chen et al. 2022). Specialized BDA networks refine these templates: BDANet inserts attention into skip paths for damage cues; BD-SKUNet adds selective-kernel modules and cascaded heads to separate mid-level classes; and RescueNet uses a joint footprint-and-damage head to reduce latency and error propagation in operational mapping (Hou et al. 2024; Shen et al. 2022; ZHAO Jinling 2024; Gupta and Shah 2021; Ahmadi et al. 2023). Transformer-based backbones, especially Swin, contribute longer-range context and benefit from self-supervised pretraining when labeled data are scarce (Cui et al. 2023). Across these families, hybrid two-stage and ensemble designs are common: a CNN (often U-Net-like) supplies per-building features that a lightweight classifier (RF/GBM) uses for grading; such late fusion helps under label scarcity and domain shift (Adriano et al. 2021; Liu et al. 2020b). Typical training/validation relies on large annotated corpora such as xBD/xView2 for pre/post VHR tiles, with reporting in IoU/F1 and imbalance-aware losses; for regional triage, Sentinel-2 (optical) and Sentinel-1 (SAR) provide open, scalable inputs, with VHR reserved for confirmation and fine-grained grading (Gupta et al. 2024; 2019; Su et al. 2020; Richards 2022).

For transferability to battlefield damage assessment, the same families are applicable but data regimes shift the preferred instantiation: under clouds, smoke, or contested releases, SAR-aware or fused optical-SAR pipelines become primary; where pre/post pairs are reliably available, Siamese change-pair models with attention tend to generalize better across events than post-only segmenters; and where labels are sparse, hybrid ensembles and self-supervised

or transfer-learned encoders improve robustness (Meyer 2019; Chen et al. 2022; Adriano et al. 2021; Dietrich et al. 2025). Event- or region-held-out evaluation and calibrated uncertainty are essential for analyst triage; ensembles have shown gains on out-of-distribution splits, and multimodal fusion remains a practical hedge against sensing gaps typical of conflict theaters (Benson and Ecker 2020; Adriano et al. 2021; Cui et al. 2023).

1.5.2.3 Battlefield damage assessment: evidence from Ukraine and beyond

Peer-reviewed Ukraine studies now outline three complementary methodological strands: fused medium-resolution screening, SAR time-series modeling at scale, and event-held-out robustness analyses with external authoritative checks. A seminal fused screening exemplar is the Kyiv study, which combined a Sentinel-1 log-ratio of backscatter change with Sentinel-2 textural features inside a built-up mask derived from public settlement/building layers, then verified outputs by qualitative WorldView checks and quantitative comparison against UNOSAT reference maps, correctly classifying approximately 58% of damaged buildings—credible performance given public, medium-resolution inputs and a triage objective (Aimaiti et al. 2022).

The second strand scales SAR beyond single events. Dietrich et al. (2025) train a Random Forest classifier (SMILE implementation inside Google Earth Engine) on per-pixel Sentinel-1 VV/VH backscatter time-series features (min, max, mean, median, std, kurtosis, skewness) computed for a fixed 12-month pre-war reference (2020) and rolling 3-month assessment windows. Pixel-wise damage probabilities are then aggregated to the object level by intersecting the heatmaps with open building footprints (Overture Maps; Microsoft Global ML Building Footprints). The team provides two Earth Engine dashboards: one to explore pre-computed maps and one to run the method on demand; users can adjust the decision threshold ("confidence threshold") via a slider to trade recall vs. precision for screening. Ground truth labels come from UNITAR/UNOSAT (destroyed/severely-damaged) annotations, and the method is designed for country-scale inference and humanitarian triage. This approach demonstrates sustained, all-weather monitoring, with public dashboards that expose both estimates and tunable uncertainty, bridging research and field practice (Dietrich et al. 2025; Gorelick et al. 2017).

The third strand focuses on out-of-domain generalization. The regime most relevant for conflict monitoring - showing that models tuned on one disaster or theater degrade on unseen events and geographies and therefore require event-held-out splits with uncertainty-aware mapping for operational credibility. Event- or region-held-out protocols better reflect deployment, revealing the generalization gap masked by within-scene splits and motivating confidence calibration for analyst triage (Benson and Ecker 2020).

Across these strands, authoritative public layers remain the anchor for external validity. UNOSAT's conflict-related maps for Kyivska Oblast (Irpin, Bucha) and other locales, produced by analysts on VHR imagery, provide independent references against which Ukraine studies calibrate precision and recall; these products also illustrate operational grading and metadata conventions that research systems can align to ("UNOSAT," n.d.).

Methodologically, Ukraine studies illustrate recurring design choices. Built-up masks drawn from global settlement layers and public building inventories constrain false positives in peri-urban vegetation and open land. The World Settlement Footprint (WSF) 2019 (10 m) and WSF-Evolution provide robust settlement extents derived from multitemporal Sentinel-1/2, while Overture/OSM/Microsoft building footprints extend to structure-level units for object-centric inference; each source has coverage and consistency caveats researchers must characterize (German Aerospace Center 2023).

At national scale, InSAR-style coherence change and amplitude statistics deliver coarse but timely localization of likely damage across thousands of settlements, with subsequent optical opportunities used to refine urban texture when clouds permit. Recent nationwide analyses track the location and timing of settlement damage across Ukraine using Sentinel-1 coherence time series, confirming the utility of SAR cadence for wide-area situation awareness (Scher and Van Den Hoek 2023; 2025).

These Ukraine-centric findings generalize to other conflict theaters and hybrid emergency contexts. Earlier conflict-mapping work demonstrated building-scale SAR time-series change analysis in Syrian cities (e.g., Raqqa), underscoring SAR's resilience to cloud/smoke and the value of temporal stability priors in degraded optical conditions (Lubin and Saleem 2019; Braun 2018). UNOSAT's city-level products and World Bank damage assessments for Aleppo/Hama/Idlib further exemplify authoritative baselines used by research systems to benchmark triage maps where field validation is infeasible during active operations Although regional case specifics differ, the common pattern - SAR-led detection complemented by opportunistic optical refinement and grounded in external authoritative checks - recurs (Joy-Fares, n.d.; Braun 2018).

1.5.2.4 Architectures and specializations: U-Net, SegNet, UNet++, V-Net, ResNet, DenseNet, EfficientNet

U-Net's encoder–decoder with skip connections established the dominant template for pixel-accurate segmentation under limited annotation. Variants such as Attention U-Net emphasize salient regions; Siamese U-Nets learn change-selective mid-level features; UNet++ narrows the semantic gap across skip paths with nested dense connections; V-Net extends to volumetric data. In remote sensing, these designs have proven effective across building extraction and damage mapping on both VHR and Sentinel-class inputs(Ronneberger et al. 2015; Oktay et al. 2018; Zhou et al. 2018; Daudt et al. 2018). UAV-based 3D reconstructions complement 2D radiometry; a notable point-cloud study achieved ≈90 % building-damage identification via supervoxel segmentation and topic modeling, demonstrating the value of geometric primitives alongside image cues (Liu et al. 2020a).

Specialized BDA networks refine U-Net backbones for ordinal labels and pre/post fusion. BDANet inserts cross-directional attention into a two-stage pre/post pipeline and has been validated both in challenge settings and in earthquake deployments (Shen et al. 2022; Xia et al. 2023). RescueNet unifies footprint segmentation and per-building grading with a localization-aware loss, demonstrating advantages over multi-stage pipelines (Gupta and Shah

2021; Gupta et al. 2024). BD-SKUNet integrates selective-kernel units and cascaded heads to separate mid-level classes more reliably on xBD and external data (Ahmadi et al. 2023) . DeepLab-family decoders and attention modules also appear in xBD workflows; several groups compare YOLO/UNet/DeepLab for combined detection-segmentation under class imbalance (Zhao et al. 2024; Neto and Dantas 2024).

Residual backbones such as ResNet enable deeper encoders without vanishing gradients, improving feature richness for subtle features (He et al. 2016). In disaster mapping, ResNet encoders are ubiquitous as plug-ins for U-Net/UNet++ decoders or for two-stage detection-classification pipelines, and pretraining on ImageNet typically stabilizes convergence under scarce labels (Gupta et al. 2024; 2019; Wang et al. 2022; Yuan et al. 2021). DenseNet promotes feature reuse and efficiency—attractive for high-dimensional inputs and when compute budgets are constrained (Huang et al. 2017). EfficientNet's compound scaling provides a tunable accuracy–efficiency trade-off, with studies noting robust cross-region transfer in change detection and production-oriented deployments where small models are advantageous (Tan and Le 2019; Adriano et al. 2021)

1.5.2.5 GANs, self-supervision, and graphs: addressing imbalance, label scarcity, and structure

Generative Adversarial Networks (GANs) are widely used to oversample underrepresented damage classes and to translate styles across sensors/disasters. xBD's class imbalance—dominated by "no-damage" and under-represented mid-level classes—has been well documented, with downstream F1 typically ordered as *no-damage > destroyed > major > minor* (Zhao et al. 2024; Gupta et al. 2019; Su et al. 2020). Studies confirmed that augmentation strategies such as cGANs and CycleGANs (Goodfellow et al. 2014; J.-Y. Zhu et al. 2017) and class-balanced sampling improve minority-class performance across multi-hazard scenarios (Su et al. 2020). Multimodal fusion—optical texture with SAR backscatter/coherence—further boosts robustness under clouds and at night, a point emphasized by both classic SAR damage studies and recent global datasets (Balz and Liao 2010; Adriano et al. 2021; Wang et al. 2019).

Self-supervised learning reduces annotation burden by pretraining on unlabeled archives. Geography-aware contrastive pretraining and spatiotemporal objectives have improved downstream accuracy and cross-event generalization for damage classification and change detection, including on xBD (Ayush et al. 2021; H. Xie et al. 2022). Transformer backbones benefit particularly from large-scale SSL when transferring across regions and sensors.

Graph Neural Networks extend beyond grid-based pixels to building/infrastructure graphs, encoding adjacency, road connectivity, or shared utilities. In damage mapping, graph-based semantic change detection and object-centric pipelines propagate context through neighborhoods, a valuable property where occlusions, smoke, or label sparsity degrade local evidence (Zheng et al. 2021). For USAR, uncertainty-aware graph integration helps rank sectors by both damage likelihood and confidence under partial ground truth (Selvakumaran et al. 2025).

1.5.3 Validation and testing

Credible battlefield and post-disaster damage assessment depends on carefully designed validation that simultaneously measures numerical accuracy, operational reliability, and uncertainty. In remote sensing, the confusion matrix remains the basic accounting tool from which precision, recall, F1, overall accuracy, and Kappa are derived, yet each metric highlights a different operational risk profile. In imbalanced settings such as building damage mapping, class-wise F1 and macro-averaged F1/IoU are preferred over overall accuracy because they prevent a dominant "no-damage" class from masking failures on rare damage categories (Congalton 1991; Sokolova and Lapalme 2009).

Where prediction targets are ordinal—no, minor, major, destroyed—evaluation should respect the order structure because confusing "destroyed" with "no damage" carries different implications than confusing "minor" with "major." In practice, this is handled either by explicitly ordinal losses during training or by reporting cost-sensitive or ordinal-aware metrics alongside standard F1/IoU, with per-class confusion matrices retained to expose asymmetric errors for analyst review (Sokolova and Lapalme 2009).

Sampling design is as important as metric choice. Random splits within one area almost always leak geographic context and inflate accuracy. Robust practice holds out entire events or regions so that test scenes differ in building typology, imaging conditions, and damage patterns; on xBD/xView2-style problems this exposes a substantial out-of-domain generalization gap between within-event and cross-event performance (Benson and Ecker 2020). In SAR-led workflows, sampling must also respect radar geometry: layover and shadow areas systematically bias backscatter and coherence and should be masked during both training and testing to avoid optimistic estimates (Plank 2014).

External, independent checks increase trust. In Europe and many international responses, analyst-curated layers from Copernicus EMS Rapid Mapping and UNOSAT are appropriate external comparators; their activation mechanisms, product taxonomies, and 24/7 analyst workflows provide a reference standard for public products even when per-building "ground truth" is infeasible in the first 24–72 hours (Chawanji et al. 2022; "Open Data Program," n.d.; "UNOSAT," n.d.). For Ukraine-related mapping, peer-reviewed work has explicitly compared fused Sentinel-1/2 outputs to UNOSAT damage maps in Kyiv, obtaining credible but imperfect agreement consistent with the medium-resolution, public-data design goals (Aimaiti et al. 2022).

Uncertainty calibration is operationally critical. Nominally high softmax scores frequently overstate correctness in modern deep networks; uncalibrated probabilities can mislead triage and tasking. Post-hoc calibration techniques such as temperature scaling and Dirichlet calibration produce more faithful probabilities, enabling reliability diagrams, expected calibration error, and thresholding strategies that align predicted confidence with observed accuracy. Calibrated outputs are particularly useful when analysts must prioritize sectors under

time pressure or when model families are fused in ensembles (Naeini et al. 2015; Guo et al. 2017).

For SAR-aware and fused pipelines, modality-specific diagnostics should be added. In amplitude/coherence time-series, stability priors and acquisition masks should be reported together with per-class F1/IoU so analysts can relate misses and false positives to unfavorable viewing geometries or decorrelation effects. In fused optical–SAR settings, ablation tables clarifying the contributions of VV/VH ratios, interferometric coherence (where SLCs exist), and optical texture features are valuable to avoid over-attribution of gains to a single sensor (Meyer 2019; Richards 2022).

Ultimately, the highest standard of validation is authoritative ground truth. In conflicts, access constraints make full field surveys infeasible during active operations. The pragmatic approach is tiered: use event-held-out splits and strong, class-wise metrics for development; calibrate and quantify uncertainty for operations; and, when available, reconcile outputs against independent analyst products from UNOSAT or Copernicus EMS and ad-hoc VHR spot-checks for qualitative confirmation ("UNOSAT," n.d.; Chawanji et al. 2022).

1.5.4 Five modeling families in current use

Bi-temporal change/damage networks process pre- and post-event imagery in parallel with weight sharing, learning contrast-selective representations that suppress illumination and seasonal artefacts. Fully convolutional Siamese designs (e.g., FC-Siam-Diff/Conc) and U-Net–based Siamese architectures consistently outperform single-temporal baselines when pairs are available (Daudt et al. 2018; Chen et al. 2022). Where labels are ordinal, cascaded heads and selective-kernel modules mitigate confusion between adjacent damage classes, exemplified by BD-SKUNet (Ahmadi et al. 2023).

Post-only segmentation/classification remains essential whenever pre-disaster imagery is missing or cannot be disseminated. Robust baselines rely on U-Net encoders such as ResNet/EfficientNet with focal-plus-Dice or class-balanced losses and aggressive augmentation; in recent xBD/XView2-style evaluations, attention-augmented variants, two-stage detectors-plus-classifiers, and transformer-assisted decoders improved minority class stability under sparse labels (Zhao and Zhang 2020; Wang et al. 2022; Gupta and Shah 2021).

Transformer/attention-centric models leverage long-range context to disambiguate clutter. Swin-Transformer backbones and Mask2Former-style decoders have reported gains for large-scale building extraction and change detection; Siamese Swin variants fuse pre/post features end-to-end, benefiting conflict scenes with repetitive urban textures (Gibril et al. 2024; Tang et al. 2024).

SAR-aware and radar-led models encode amplitude series, co- and cross-pol ratios, and, where SLCs exist, interferometric coherence as stability priors. Polarimetric intuition is often embedded implicitly: co-pol channels accentuate double-bounce from façade–street canyons;

cross-pol emphasizes vegetation volume; their ratios support urban/non-urban separation. Authoritative tutorials and handbooks remain standard references (Van Zyl and Kim 2011; Meyer 2019; Richards 2022), while Ukraine work demonstrates public, scalable pipelines that combine SAR change cues with optical texture and built-up masks (Aimaiti et al. 2022).

Lightweight and uncertainty-aware graph methods address the first 24–72 hours when labels and compute are scarce and triage maps with explicit confidence are more actionable than hard classifications. Message-passing over building graphs, belief propagation, and subjective-logic uncertainty quantification expose unreliable regions for analyst review, complementing heavier CNN/transformer models in fast-moving crises (Selvakumaran et al. 2025).

1.5.5 Synthesis: matching models to regimes

When fast, public triage is needed over wide areas, SAR-led or fused pipelines with light-weight classifiers and confidence maps are appropriate, exploiting Sentinel-1 time series and opportunistic Sentinel-2 texture, validated against UNOSAT or Copernicus EMS layers and spot VHR. When pre/post pairs are reliably available and releasable, Siamese encoder–decoders with attention blocks and ordinal heads remain the backbone for graded damage. For post-only conditions in contested access, single-temporal U-Net/UNet++ with strong encoders, imbalance-aware losses, and SSL pretraining provide robust baselines. Across regimes, graph-level reasoning and human-in-the-loop uncertainty review align model outputs with operational decision-making, especially in the first 24–72 hours.

1.6 Systematic Challenges

- **Data Scarcity and Heterogeneity:**
  Urban morphologies, conflict types, and damage patterns are highly variable in Europe; open data is often limited for recent conflicts.
- **Cloud Cover and Adverse Imaging Conditions:**
  SAR is critical to overcome persistent cloud cover and to complement optical gaps, especially in combat zones.
- **Label and Domain Transfer:**
  Harmonization of disaster- and conflict-derived datasets and transferability of models remains a challenging research frontier.
- **Scalability and Real-time Deployment:**
  Model compression, efficient architectures, and high-speed inference are necessary for operational use (e.g., defense and civil response).
- **European Morphology Bias**: Most datasets are non-European, requiring adaptation.
- **Cross-Domain Transfer**: Conflict vs. disaster damage differ in spatial/temporal signatures.
- **Infrastructure Beyond Buildings**: Roads, bridges, and pipelines need dedicated model branches.
- **Data Imbalance**: “Destroyed” classes areunderrepresented.

The operationalization of remote sensing and artificial intelligence for battlefield damage assessment of urban structures faces a series of intertwined challenges that span data, methodology, scalability, and ethics. A central issue is data scarcity and heterogeneity. Urban morphologies in Europe differ substantially from those represented in widely used disaster datasets such as xBD, which—despite covering over 850,000 annotated buildings across multiple hazards—remains dominated by non-European architectures and suffers from severe class imbalance (Gupta et al. 2019; Su et al. 2020; Braik and Koliou 2024). The underrepresentation of “destroyed” and mid-level damage classes has been shown to degrade performance, with F1 scores consistently ranking no-damage highest, followed by destroyed, major, and minor categories (Benson and Ecker 2020; Su et al. 2020). Augmentation methods including generative adversarial networks, CutMix, and semi-supervised autoencoder pretraining reduce these biases and improve model generalizability when annotations are sparse (Li et al. 2018a; Hao et al. 2023; Mueller et al. 2021). Nevertheless, harmonizing disaster-derived and conflict-derived datasets, with their differing temporal and spatial signatures, remains a persistent frontier.

Adverse imaging conditions constitute a second obstacle. Optical satellites are frequently constrained by cloud cover, smoke, or debris in conflict zones, while SAR—although indispensable for all-weather, day-night coverage—introduces challenges of speckle, geometric distortion, and complex scattering that require specialized preprocessing and model adaptation (Flores et al. 2019). Integrating multi-modal observations through fusion of SAR

and optical imagery has shown strong potential for mitigating these limitations, particularly when coupled with open geospatial layers such as building footprints or transport networks (Aimaiti et al. 2022; Adriano et al. 2021).

A further challenge lies in scalability and real-time deployment. Deep models such as U-Net, BDANet, and ResNet-based pipelines provide high segmentation accuracy but remain computationally expensive, especially for very-high-resolution inputs and national-scale monitoring (Ronneberger et al. 2015; Gupta et al. 2019; Shen et al. 2022). Model compression, efficient architectures such as EfficientNet, and GPU-accelerated cloud deployment are critical to bridge the gap between research prototypes and operational systems (Tan and Le 2019; Dietrich et al. 2025). These requirements are especially acute in European defense contexts, where actionable information must be delivered within hours rather than days.

Finally, technical progress must be balanced with ethical and policy considerations. High-resolution satellite imagery over war zones raises questions of privacy, sovereignty, and the potential misuse of surveillance outputs. While studies demonstrate the value of conflict-aware monitoring for humanitarian response and reconstruction planning (Butenko and Petrychenko 2023; Holail et al. 2024), scholars also caution against the risks of escalation or rights violations if such tools are not embedded within transparent governance frameworks (Mueller et al. 2021). Interpretable architectures, uncertainty-aware mapping, and interactive platforms that expose model limitations are thus essential for responsible use in high-stakes environments (Cao and Choe 2024; Xie et al. 2020; Selvakumaran et al. 2025).

1.7 Knowledge Synthesis and Research Trends

Recent developments reflect a rapidly evolving field that integrates remote sensing and artificial intelligence into operational frameworks for urban damage assessment. Al Shafian and Hu (2024) provide a bibliometric analysis of 370 studies published between 2014 and 2024, identifying thematic clusters in sensor fusion, model architectures, and operational deployment, while also highlighting persistent gaps such as limited attention to European urban morphologies and real-time applicability (Al Shafian et al. 2025). Complementing this macro-level synthesis, Taiwo H. Agbaje et al. (2024) examine practical challenges in deploying GeoAI for building damage detection, emphasizing bottlenecks in data availability, annotation quality, and the reliability of transfer learning under operational constraints (Taiwo H. Agbaje et al. 2024). Earlier work by Lubin and Saleem (2019) already underscored structural limitations in the field, particularly issues of cloud cover, multi-source data fusion, explainability of AI predictions, and the ethical risks of remote sensing in conflict zones (Lubin and Saleem 2019). Taken together, these studies map the state of the art, demonstrating both the accelerating technical progress in automated and context-aware systems and the need for governance structures that ensure ethical, standardized, and operationally relevant deployment in disaster and battlefield contexts.

1.8 Conclusion

The combined use of remote sensing (RS) and machine learning (ML) has transformed the practice of urban damage assessment in both post-disaster and conflict environments. Advances in very-high-resolution satellite imagery, SAR–optical data fusion, and deep learning architectures such as U-Net and transformer-based models have enabled scalable, rapid, and increasingly precise mapping of structural damage. Automated pipelines now make it possible to classify and rank affected buildings with efficiency that supports humanitarian relief, reconstruction planning, and conflict monitoring.

Despite this progress, several research gaps remain critical. Domain generalization is still a major limitation: models trained in one geography or disaster type often degrade when transferred to new contexts with different architectural forms or conflict dynamics. Data scarcity—especially the absence of reliable pre-disaster imagery in active war zones—further constrains training and evaluation. Ethical challenges, including risks of surveillance misuse, privacy violations, and geopolitical sensitivities around high-resolution mapping, remain insufficiently addressed. Finally, there could be a lack of integrated frameworks that unify damage detection and decision-support functions into interpretable, trustworthy systems. Closing these gaps will be essential to establish resilient, adaptable, and ethically robust solutions for future urban disasters and battlefield monitoring.

2 Appendix

2.1 Research Framework and Methodological Foundations

2.1.1 Scope and Purpose

This literature review systematically examines recent advances at the intersection of remote sensing, satellite-based image analysis, GIS/geoinformation science, and machine learning relating to the topic of **«battlefield assessment of urban structures with remote sensing and machine learning in European conflict zones»**.

The goal is to provide a comprehensive foundation for the master's thesis and a potential academic publication on the integration of multimodal remote sensing data—particularly SAR and RGB imagery—with advanced deep learning techniques for damage assessment in European conflict and disaster zones. Special emphasis is placed on practical feasibility and operational implementation within existing infrastructures. The envisioned workflow ingests pre- and post-disaster imagery, applies machine learning (ML) models for analysis, and generates polygons with damage ratings based on the European Macroseismic Scale (EMS-98) for visualization in GIS applications such as QGIS.

2.1.2 Working Title for Masterthesis

"Battlefield Damage Assessment in European Conflict Zones Using Multimodal (RGB + SAR) Satellite Images and Deep Neural Networks."

2.1.3 Scientific Research Questions

How can the integration of multi-modal remote sensing data - specifically Synthetic Aperture Radar (SAR) and high-resolution optical imagery - be leveraged with advanced machine learning techniques to enable scalable, robust, and near real-time assessment of urban infrastructure damage following military conflict or natural disasters in European settings, while providing interpretable and actionable outputs directly within operational GIS platforms?

Scientific Research Subquestions

Pre- and Post Disaster Remote Sensing Data

How can pre- and post-disaster remote sensing data be effectively utilized in deep learning frameworks (e.g., convolutional neural networks or pretrained architectures) for accurate urban infrastructure segmentation and damage assessment?

SAR and Optical Data Fusion:

How effective is the fusion of SAR and optical data for damage classification in European urban morphology?

Dataset Integration:

What are the challenges and best practices for combining open-source datasets from conflict and disaster zones?

ML Methods

Which machine learning methods are most suitable for the segmentation of urban structures and the reliable classification of structural damage in post-disaster scenarios?

Model Transferability:

How transferable are models trained on natural disaster data to military conflict scenarios, and vice versa?

Integration into GIS

How can deep learning-based urban damage models be integrated into GIS platforms to provide spatially explicit, interpretable, and actionable damage maps?

2.1.4 Search Strategy and Selection Criteria

Sources

Name	Type	Example Journals / Articles	URL
Google Scholar	Academic Search Engine / Metadata Index	Broad indexing of all academic content; used for literature search	https://scholar.google.com
ResearchGate	Academic Repository / Network	Preprints, postprints, early versions of published journal articles	https://www.researchgate.net
MDPI	Open Access Publisher	Remote Sensing, Buildings, Water, Sensors	https://www.mdpi.com
IEEE / IEEE Xplore	Publisher / Conference Repository	IEEE Access, IEEE Geoscience and Remote Sensing Letters, conference papers from MIPR, IRI, etc.	https://ieeexplore.ieee.org
Springer / Springer Nature	Academic Publisher	Natural Hazards, International Journal of Disaster Risk Science, conference proceedings	https://link.springer.com
Elsevier / ScienceDirect	Academic Publisher	International Journal of Applied Earth Observation and Geoinformation, Automation in Construction	https://www.sciencedirect.com
Oxford Academic (Oxford University Press)	Academic Publisher	National Science Review	https://academic.oup.com
IAES (Institute of Advanced Engineering and Science)	Academic Publisher	IAES International Journal of Artificial Intelligence (IJ-AI)	https://iaescore.com/journals/index.php/IJAI
IOP Publishing	Academic Publisher	IOP Conference Series: Earth and Environmental Science	https://iopscience.iop.org
SPIE Digital Library	Scientific Publisher	Journal of Applied Remote Sensing	https://www.spiedigitallibrary.org
Ingenta Connect	Aggregator / Journal Hosting Platform	Provides access to titles like Photogrammetric Engineering & Remote Sensing	https://www.ingentaconnect.com
scite	AI Tool for Scientific writing	AI citation platform	https://scite.ai

Tabelle 1: Sources for literature research with URLs

1. Application-Specific Terms

- war damage assessment
- battlefield damage assessment
- post disaster damage assessment
- post earthquake damage assessment
- conflict monitoring
- conflict damage detection
- post-war urban reconstruction
- infrastructure damage mapping
- building damage classification
- structural damage detection
- change detection in conflict zones

2. Methodological & ML Terms

- deep learning
- DNN
- deep neural network
- convolutional neural network
- CNN
- Siamese network
- transformer model
- vision transformer
- ViT
- semantic segmentation
- instance segmentation
- object detection
- domain adaptation
- transfer learning
- data fusion / multimodal fusion

3. Remote Sensing / Data Terms

- satellite imagery
- synthetic aperture radar
- SAR
- InSAR
- interferometric SAR
- polarimetric SAR
- PolSAR
- Satellite
- Remote Sensing

- Optical Satellites
- very high-resolution (VHR) imagery
- open-source damage datasets (e.g., xBD, UNOSAT)

4. Operational / GIS Integration Terms

- GIS-based damage mapping
- geospatial AI / GeoAI
- decision support systems
- rapid mapping
- near real-time damage assessment
- emergency response mapping

Selection Criteria

- **Date Range:**
  works published from **2000 onward** were preferred, except for primary scientific literature.
- **Language:**
  Only publications in **English** were included.
- **Geographical Focus:**
  Preference was given to studies with a focus on **Europe** and Western urban structures. However, work from other global regions was included wherever the methodologies or datasets were applicable or generalizable.
- **Type of Source:**
  The research focused on peer-reviewed papers and journal articles, reputable conference proceedings, well-recognized preprints, and scholarly book chapters.
- **Exclusion:**
  Publications in other languages, works prior to 2000, studies focused solely on rural or non-urban applications unless offering transferable methodologies, and non-scholarly reports without rigorous methodology.

Assessment of Quality and Relevance

To ensure both scientific best practices and practical relevance, the following criteria were applied during source evaluation:

- **Publication Venue:**
  Priority was given to articles published in major, peer-reviewed outlets such as Springer, MDPI, Nature, and other respected journals.
- **Citation and Impact:** Preference was shown to sources whose authors were cited elsewhere in the literature, demonstrated through reference mapping or bibliometric tools.

- **Conference Participation:** Studies authored or presented at recognized international conferences were included, as such venues often signal community validation and fresh insights.
- **Data Source Transparency:** Articles that clearly detailed their datasets, data availability, and reproducibility measures (e.g., code repositories, dataset documentation) were prioritized.
- **Relevance to Research Question:** Works directly addressing the intersection of *machine learning, remote sensing, and rapid damage assessment*—especially for urban and battlefield scenarios—were emphasized.
- **Methodological Rigor:** Sources describing robust experimentation, ablation studies, comparative benchmarking (e.g., with xBD Dataset), and quantitative performance metrics (IoU, F1-score, etc.) were considered highly valuable.

2.1.5 Search and Identification of Literature

The defined search terms and their combinations were primarily applied in **Google Scholar** but also used within the search portals of major publishers (IEEE Xplore, SpringerLink, ScienceDirect, MDPI, Oxford Academic, SPIE, IOP, and others). After an initial exploratory search, approximately 20 key papers were identified as highly relevant to the research topic. The reference lists of these publications were then systematically examined, which led to further expansion of the search terms and identification of additional relevant literature.

2.1.6 Literature Workflow

All identified papers and related works were imported into **Zotero** for structured management. As the search expanded iteratively through database queries and reference snowballing, the final corpus reached **194 papers**. For each paper, a dedicated Zotero note was created following a standardized structure designed to ensure consistency and enable downstream processing.

The structure of each note included bibliographic and descriptive metadata (title, type, publisher, year, DOI, links, and authorship), as well as extracted information on keywords, datasets, satellites, models, and methodologies. Where possible, bibliographic metadata were retrieved from BibTeX entries or directly extracted from the paper. Local metadata (e.g., PDF location, file type, and publication details) were added manually.

Summaries and structured extracts were produced in multiple steps:

- **Abstracts and metadata** were imported or extracted via BibTeX and Adobe Acrobat Pro's AI metadata tools.
- **Summaries of context, objectives, data, methods, results, and recommendations** were generated using the Adobe Acrobat AI Assistant to provide structured overviews.
- **Referenced paper lists** were copied manually and subsequently normalized into a numbered list using PowerShell scripting to ensure uniform formatting across all notes.

All Zotero notes were then **exported as Markdown files**, providing a machine-readable and interoperable format. This export served as the input for a set of **Python scripts**, written by the author and iteratively enhanced with the support of ChatGPT-4 and ChatGPT-5, which automated further normalization, enrichment, and cross-referencing of the literature database.

2.1.6.1 Python Quick map (001–015)¨

See detailed Code description in Appendix.

- **001_unicode** — Normalize Unicode/line endings; keep H1 + "## Abstract" backbone; drop noise between H1 and Abstract.
- **002_html_remover** — Strip HTML safely; keep URLs; convert block tags to line breaks.
- **003_only_summary** — Re-anchor Abstract after H1, scaffold **Summary** trio, move **Referenced Papers** to end.
- **004_bold_to_h3** — Convert bold **Field:** to canonical ### Field: inside ## Metadata / ## Extracted Data.
- **005_references_to_numbered_list** — Rebuild **References** as a clean 1. list (multi-line aware).
- **006_satellites** — Parse "Which Satellite Used" + free text; insert ## Satellites found: with modality (SAR/optical); JSON/CSV QA.
- **007_dataset_scraper** *(discovery)* — Read-only pass; discover datasets from the section and body; write JSON/CSV, no edits.
- **007_dataset_scraper** *(insertion)* — Insert **### Datasets parsed:** right after ### Dataset Used:; exclude References; annotate kinds.
- **009_keywords** — Build YAML tags: + visible ### Tags: from **Keywords**, **BibTeX**, **Satellites**, **Datasets** (+ corpus-freq optional cues).
- **010_bibtex_fence** — Fence the region **between** ## Bibtex Metadata and ## Metadata as ```bibtex.
- **011_URL** — Plain URLs only; canonicalize DOIs; annotate unreachable links; CSV audit.
- **012_DOI** — Fill missing DOIs **only** in References via Crossref/DataCite/PubMed; CSV audit + JSON cache.
- **013_Zotero** — Insert ## Linking between BibTeX/Metadata; upsert YAML with Zotero URIs and citation key.
- **014_obsidian** — Append ## Tags (obsidian) with per-tag related-note links using YAML tag overlap.
- **015_references_linking** — Append ## References (obsidian) with backlinks to in-vault notes (DOI→file; else Title→file).

This normalization enables automatic aggregation of core evidence across the corpus—benchmark datasets (e.g., xBD, SpaceNet, LEVIR-CD), satellites/sensors (e.g., Sentinel-1/2, WorldView, TerraSAR-X, ALOS-2), and ML models (e.g., U-Net variants, Siamese nets,

transformers, ensembles)—and exposes them as machine-readable sections and tags. The tag layer then powers Obsidian cross-links, letting related notes surface instantly and supporting graph-based exploration to identify pivotal papers (high centrality and high reuse of datasets/methods) and to trace the newest/best-performing approaches across time, modality, and task (segmentation vs. change detection vs. ordinal damage classification). In turn, this structured view underpins the derivation of the study's own methodology: selecting representative datasets, choosing sensor pairs (RGB+SAR) and fusion strategies, prioritizing model families and training regimes (transfer learning, augmentation), and defining robust evaluation criteria (IoU/F1, OOD generalization, operational latency).

2.1.7 Python Note Processing Pipeline

Note Structure before preprocessing

TITLE

Abstract:

Bibtex Metadata:

Metadata

Title:

PDF:

PDF Local:

Type:

Publisher:

If Journal or Conference Paper, Title of Journal, Title of Conference:

Year:

Date published:

Link:

Link https:

DOI:

All Authors:

Extracted Data:

Keywords:

Code Available At:

ML Model Used:

Remote Sensing Imagery Used:

Which Satellite Used:

Dataset Used:

Methodology Used:

Summary:

Summary: Context and Objective

Summary - Data and Methods

Methods

Tools

Application

Summary - Results, Conclusion, and Recommendations

Results

Conclusion

Recommendations

Referenced Papers

Normalization of Notes via Python Pipeline

Below is an in-depth, script-by-script description of the Python literature-processing pipeline. Documentation and Description of Code done via ChatGPT 5.

2.1.7.1 001_unicode.py (Markdown Unicode normalization + heading cleanup)

Role in pipeline:

This is the very first "hygiene" pass over the raw Markdown export. It both normalizes Unicode (for search/indexing stability) and enforces a clean document preamble: keep the first # H1 and the first ## Abstract that follows; remove everything between them.

What it does:

- Normalization: converts CRLF/CR → LF; NFKC normalizes; strips BOM/zero-width characters; turns NBSP/NNBSP into normal spaces; discards other control chars except \n/\t; trims trailing spaces per line.
- Structure cleanup: finds the first H1 and the first "## Abstract" *after* that H1; removes all lines strictly between them and ensures exactly one blank line in between afterward.

- Idempotent by design: re-running won't perform further changes.

Key points & regexes:

- H1_RX, H2_RX find first-level headings; _normalize_heading_name() collapses heading noise (trailing colon, parens/spaces) to match "Abstract" robustly.
- If there's no H1 or no Abstract after the H1, it leaves structure intact and only normalizes Unicode.
- Walks a source tree and mirrors it to an output tree (DEFAULT_SRC_ROOT → DEFAULT_OUT_ROOT) with consistent \n line endings.

All later scripts depend on consistent headings/whitespace and plain ASCII spaces; this guarantees predictable parsing and regex matches across the corpus.

2.1.7.2 002_html_remover.py (strip embedded HTML, preserve hrefs)

Role in pipeline:

Many notes carry HTML fragments (copied references, rich pasted text). This pass removes HTML while preserving semantics (links, block breaks).

What it does:

- Replaces … with just the href URL so no information is lost.
- Converts
 and block-closing tags (</p>, , , …) into newline(s); strips all other tags; decodes HTML entities.
- Collapses trailing spaces and excessive blank lines.

Key patterns:

- ANCHOR_RX, BR_RX, BLOCK_CLOSE_RX, TAG_RX handle most HTML; the strip_html function applies them in a safe order.
- Operates in-place over a mirror root (defaults to your temp working dir).
- Quick skip: if a file contains no <, it's not scanned further.

Downstream regex-based sectioning (e.g., Metadata/Extracted Data, References) is brittle when angle-brackets/HTML leak into the Markdown; this step makes content consistently Markdown-only.

2.1.7.3 003_only_summary.py (re-anchors Abstract/Summary and scaffolds metadata blocks)

Role in pipeline:

This script canonicalizes the top-of-file layout and ensures the "metadata scaffolding" is present whenever the first section was a "Summary". It also standardizes the three Summary sections expected later.

What it does:

- Splits off YAML front matter if present, tidies blank artifacts.
- Extracts the Abstract (from anywhere), removes it, and reinserts it immediately after the H1 as ## Abstract:.
- If the first H2 after H1 was originally “Summary”, it injects a pre-block right after Abstract containing the headers for BibTeX/Metadata/Extracted Data.
- Ensures the canonical trio of Summary sections exists (create if missing):
  - ## Summary: Context and Objective
  - ## Summary - Data and Methods (with ### Methods | Tools | Application)
  - ## Summary - Results, Conclusion, and Recommendations (with ### Results | Conclusion | Recommendations)
- Moves “## Referenced Papers” to the very end, collapsing duplicates.

Key logic:

- Robust header matching (ABSTRACT_H2, SUMMARY_H2, CTX_H2, DM_H2, RCR_H2, REFS_H2) including case/colon variants; create if missing, and ensure required ### subheads exist (or append them).
- Minimal whitespace tidy and re-assembly with the original (or preserved) YAML front matter.

This guarantees a uniform “spine” (H1 → Abstract → [optional Pre-Block] → Summary sections → rest → Referenced Papers), which later scripts rely on to insert/normalize fields.

2.1.7.4 004_bold_to_h3.py (normalize “Metadata” / “Extracted Data” fields to H3 blocks)

Role in pipeline:

Many exports render fields as bold lines (**Title:**) mixed with ### headings; this pass converts those into consistent ### Field: blocks inside ## Metadata and ## Extracted Data: sections.

What it does:

- Accepts both ## Metadata or bare Metadata lines; same for Extracted Data.
- Parses both bold-marker fields and H3 fields (**Label:** … or ### Label: …), consolidates them into normalized blocks:
- ## Metadata
- ### Title:
- <content>
- Keeps inline remainder values (after the label on the same line) and the subsequent paragraph up to the next field as the field content; strips stray “summary” lines that leaked into these sections.

- Rewrites the section header line and field blocks in a consistent order without touching content.

Key regexes:

- BOLD_ANY and H3_ANY capture field labels and inline values; BAD_SUMMARY drops leak artifacts; HDR_LINE recognizes section headers with or without ##.
- Rebuild is stable/idempotent; reruns won't churn.

Later automation depends on finding ## Metadata / ## Extracted Data: and ### fields unambiguously (e.g., for downstream scraping, tagging, or QA).

2.1.7.5 005_references_to_numbered_list.py (rebuild clean numbered References)

Role in pipeline:

References lists are often inconsistent: mixed numbering styles, broken lines, or unnumbered text. This pass converts the References block into a clean sequential "1. …" list, preserving content.

What it does:

- Locates a references section by common headers: References, Referenced Papers, Bibliography, Literature.
- Detects style (e.g., 1., 1), [1], or none) and parses multi-line entries robustly.
- Rebuilds an ordered list with 1. …, 2. …, etc., without touching the internals of each reference item.

Key regexes & heuristics:

- HEADER_RX finds the block; NUM_RX, BRACK_RX match numbered/bracketed forms; START_REF_RX heuristic helps segment unnumbered references (capitalized author + year pattern).
- Writes to a separate out-root; safe to rerun.

Clean, consistently numbered references are easier to post-process (e.g., dedupe, DOI checks) and won't confuse dataset/keyword scanners that must avoid the References region.

2.1.7.6 006_satellites.py (canonical satellite extraction + "Satellites found" block)

Role in pipeline:

Extracts canonical satellite names (and their modality: SAR/Optical/Other) from both a standard "Which Satellite Used" section and free text. Inserts a machine-readable block upstream of dataset processing.

What it does:

- Normalization: NFKC + zero-width stripping at tokenizer level to make fuzzy strings matchable.
- Structured pass: if a ##/### **Which Satellite Used** block exists, parse bullets and expand shorthand like ERS-1/2/3, SPOT 6/7, Sentinel-1A/B(/C).
- Aliases: large alias→canonical map (e.g., ETM+ → Landsat-7; WV2/WV3; TerraSAR-X; RADARSAT; ALOS-2 PALSAR-2, etc.).
- Full-text pass: scans entire note using token regexes (RE_TOKEN, RE_DASH_SUFFIX) and descriptor stripping; assigns canonical names when possible.
- Insertion: writes/updates a ## Satellites found: block (one per file) with - <Canon>, <Modality> before ### Dataset Used if found, otherwise at EOF.
- Reporting: also writes JSON (per file) and CSV (hit-level with match type and modality) for QA.

Key strengths:

- Robust to hyphen shorthand (WorldView-2 and -3) and noise words (“imagery”, “data”, “sensor”).
- Keeps originals untouched; writes to an output tree mirroring the input.

These canonical satellites and their modality feed your keyword tagging and fusion detection, and are later surfaced in Tags as mandatory tokens (e.g., sar, optical).

2.1.7.7 007_01_dataset_scraper.py (read-only dataset discovery + logging) (discovery version)

Role in pipeline:

A read-only pass to mine dataset names from (a) the ### Dataset(s) Used section (source of truth) and (b) the whole note using a seed alias catalog without modifying files. Produces JSON/CSV for QA and catalog growth.

What it does:

- Section canonicalization: trusts the exact strings listed under ### Dataset(s) Used as canonical per file.
- Global discovery: scans full text for known aliases (e.g., xBD/xView2, SpaceNet, ISPRS Potsdam/Vaihingen, Inria Aerial, LEVIR-CD, SZTAKI AirChange, BigEarthNet, SRTM, WorldCover, Dynamic World, Microsoft/OSM footprints, UNOSAT, ARIA DPM).
- Heuristics: looks for *Named Phrase + keyword* or *keyword: Named Phrase* patterns (e.g., “LEVIR dataset”, “dataset: Inria Aerial”), with noise trimming and stop-word/stop-tail filtering.
- Conflict resolution: if a catalog alias maps to a canonical name that already appears verbatim in the section, the section spelling wins.
- Outputs: per-file JSON and a CSV of candidates with counts; prints top datasets and unknowns (to expand the catalog later).

Getting acorpus-wide picture of which datasets are used—even if authors forgot to fill the Dataset Used section—before modifying notes or inserting blocks.

The repository includes another dataset script with *insertion* behavior (below) used as Step 008. Although both files share the 007_1*.py and 007_2*.py name in the headers, they are used them in sequence as 007 (read-only) then 008 (insertion).

2.1.7.8 007_2_dataset_scraper.py (insert "### Datasets parsed:" after "Dataset Used") (insertion version)

Role in pipeline:

A write-back pass that inserts a ### Datasets parsed: block directly after ### Dataset Used: and before ### Methodology Used (with fallbacks), consolidating section-listed datasets and extra discoveries (excluding References).

What it does:

- Hard guarantees:
    1. Treat "### Dataset Used:" as canonical (verbatim).
    2. Exclude any "References/Referenced Papers/Bibliography" from discovery.
    3. Map catalog aliases → canon only on the filtered (non-references) text.
    4. Strict heuristics drop sentence-like noise (e.g., "In the …").
    5. If the catalog canon is already covered by the section, do not add it again.
    6. Insert a new ### Datasets parsed: block immediately after "Dataset Used" and before "Methodology Used"; remove a prior "Datasets parsed" block if present.
- Kinds: It ships with a "kind" map (Benchmark/DEM/Product/Land Cover/Footprints/Labels/SAR-OD, etc.) and prints as - <Name>, <Kind>. Section items keep their verbatim display; extras are canonicalized.
- Writes copies to the out-dir (originals untouched) and logs JSON/CSV with the union list per file.

This gives every note a machine-readable inventory of datasets (author-declared + discovered), placed at a standardized location to support QA, tag extraction, or corpus stats.

2.1.7.9 009_keywords.py (corpus-aware tag extractor/normalizer)

Role in pipeline:

Builds a clean ### Tags: section and YAML tags: for each note by merging mandatory sources (Keywords/BibTeX/Dataset Used/Satellites) and optional cues (models/fusion/aliases) with a document-frequency gate.

What it does:

- Placement rule: insert ### Tags: below the Keywords section and before "Code Available At"; if absent, append at EOF. Remove any existing ### Tags: block first.

- Do not scan inside References.
- Mandatory tag sources (always keep):
  - BibTeX keywords (keywords={...}) anywhere outside References.
  - Keywords section (bullets or bold inline).
  - All concrete satellites found (from earlier “Satellites found:” and free-text scan) + their modality tokens (sar, optical).
  - Canonical dataset names listed under ### Dataset Used:.
- Optional sources (kept if doc-frequency ≥ --min-freq, default 2):
  - “Datasets parsed” (left-side of first comma, canonicalized), corpus-wide dataset alias hits in body (outside refs).
  - ML model regexes (cnn, unet, transformer, resnet, densenet, svm, rf, xgboost, lstm, rnn, siamese) and fusion cues.
  - Generic canonical tokens (remote sensing, optical, sar, fusion) if present in mandatory text.
- Normalization: tags are kebab-case, ≤4 words, no underscores; YAML tags: list is updated; visible ### Tags: shows a comma-separated list in kebab-case.
- Two-pass corpus logic: first collects bodies (without References) to compute global frequencies, then writes files using the min-freq threshold to filter non-mandatory tags; mandatory tags always pass.

This ensures the notes carry a consistent, deduped, query-friendly taxonomy for Dataview/Obsidian or downstream analytics, while giving weight to tags that actually recur across the corpus.

2.1.7.10 010_bibtex_fence.py (BibTeX block fencing & normalization) (file not provided)

Purpose:
Ensure that whatever content sits between ## Bibtex Metadata: and ## Metadata is a single, clean ```bibtex fenced block. This prevents downstream tools (parsers, exporters, linkers) from misinterpreting BibTeX as prose.

Inputs/Outputs:

- **Input:** Markdown notes (YAML front-matter respected).
- **Output:** Mirrored Markdown copies with a normalized fenced BibTeX block between ## Bibtex Metadata: and ## Metadata. If the region is empty/malformed, an **empty** fenced block is inserted for structural stability.

Core logic:

- Detect the **start** (## Bibtex Metadata — case/colon tolerant) and the next ## Metadata as **end boundary**.
- If the captured region is already fenced (any fence flavor), unwrap and re-wrap to normalize to:

- ```bibtex
- @article{…}
- Collapse runs of ≥3 blank lines inside the fenced portion to a single blank line.

Idempotency & edge cases:

- If no ## Metadata header appears **after** ## Bibtex Metadata:, the file is left untouched (explicit boundary safety).
- Re-running is safe: the fenced region won't change and no extra fences will be added.

A guaranteed machine-parsable BibTeX region avoids breakage in later steps (DOI harvesting, Zotero linking, exports) and ensures consistent structure across the corpus.

2.1.7.11 011_URL.py — Link normalizer + reachability auditor (plain URLs only)

Purpose:
Apply URL hygiene across the entire note:

- Convert all Markdown links [text](https://…) to plain URLs (no brackets).
- Canonicalize all DOI forms to https://doi.org/<DOI>.
- Check for reachability; annotate failures with [NOT REACHABLE] (do not delete).
- Emit a CSV audit of (file, url, status, detail) for QA.

Inputs/Outputs:

- Input: Markdown notes.
- Output: Mirrored copies with normalized plain URLs; a link-status CSV log in --log-dir.
- Idempotent post-conditions: no duplicate annotations or re-wrapping on reruns.

Core logic:

- Mask code fences first so code snippets remain untouched.
- Replace Markdown links, unwrap <angle>… URLs, fix common typos (e.g., http://examplecom → .com).
- DOI normalization: detect DOI tokens/URLs and rewrite to https://doi.org/<DOI>; optionally confirm DOI existence (e.g., via Crossref) to avoid bad rewrites.
- Reachability: HEAD with retry/backoff, fallback to GET on 405; annotate only on persistent failure.

Idempotency & edge cases:

- Big-publisher blocking/robot rules are handled conservatively; DOI canonicalization is applied even when landing pages are blocked.
- Mask/unmask of code blocks ensures zero edits inside code fences.

Plain URLs were explicitly used throughout the notes (Markdown link syntax caused issues). This step gives consistent link formatting and a one-shot, auditable link-health report.

2.1.7.12 012_DOI.py — DOI resolver for the References section (precision > speed)

Purpose:
Operate only inside ## References / ## Referenced Papers / ## Bibliography to:

- Keep and normalize existing DOIs.
- Where missing, extract (title, first author, year) and query external services (e.g., Crossref, DataCite, PubMed) to retrieve a high-confidence DOI.
- Update the References in the output copies; write a CSV audit and JSON cache for later reruns.

Inputs/Outputs:

- Input: Markdown notes.
- Output: Mirrored copies with normalized/completed DOIs in the References; CSV audit and JSON cache (to avoid repeated lookups).

Core logic:

- Robust section slicing; pack multi-line reference entries reliably.
- Title extractor avoids URLs/DOIs, supports quoted titles, and stops at typical journal tokens (Journal/Transactions/Proceedings/ISPRS/etc.).
- Matching policy: accept matches with strong prefix or high similarity ratio; allow author/year soft checks to disambiguate when close.

Idempotency & edge cases:

- Year bounds to reduce noise (e.g., 1950–2025).
- Existing short DOIs are preserved.
- Network-free fallback: if HTTP libraries aren't available, skip lookups gracefully (no changes).

This stage completes the reference metadata without touching the main body. Filled-in DOIs improves downstream cross-linking.

2.1.7.13 013_Zotero.py — Zotero linking between BibTeX and Metadata (YAML + visible block)

Purpose:
Finds each note's parent Zotero item and its matching child note using your BetterBibTeX JSON (primary) and optional CSL JSON (fallback for citation key). Then:

- Upsert YAML keys: citationkey, zotero_uri, zotero_item_link, zotero_bbt_link, zotero_parent_item_id, zotero_pdf_url, zotero_attachment_uri, notes_key, notes_parentItem, notes_uri.
- Insert a visible ## Linking section (H3 fields; value on the next line) between ## Bibtex Metadata: and ## Metadata.

Inputs/Outputs:

- Input: Notes, --bbt (BetterBibTeX JSON), optional --csl (CSL JSON).
- Output: Mirrored copies with YAML augmented and a visible ## Linking block in the intended slot. Idempotent on reruns.

Core logic:

- Match priority: (1) child note H1 in BBT → (2) YAML citationkey → (3) Metadata DOI → (4) Metadata title → (5) fuzzy title match.
- Attachment discovery: expose the first PDF-like attachment or zotero://select URIs for quick navigation.
- Remove any prior ## Linking block before reinsertion.

Idempotency & edge cases:

- Notes lacking H1 or BBT hits are mirrored unchanged.
- YAML quoting is robust for punctuation/spaces.

Gives round-trip traceability between Obsidian notes and Zotero items (both YAML + visible block), so you can cite and retrieve PDFs with a single click.

2.1.7.14 014_obsidian.py — Build "## Tags (obsidian)" cross-links by tag overlap

Purpose:
Turns YAML tags: into a related-notes section that shows, for each tag, the other notes sharing it, e.g.:

Tags (obsidian)

- sar [[NoteA|001]], [[NoteB|002]]

- sentinel-1 [[NoteC|001]]

- etc

Inputs/Outputs:

- Input: The full input root; script builds two indices: file → tags (from YAML front-matter) and inverted tag → [files].
- Output: Mirrored copies with ## Tags (obsidian) appended to EOF (after removing any prior managed block).

Core logic

- YAML parser supports inline lists, comma-lists, and block lists for tags:.
- Related files exclude "self".
- Ordering is stable: a note's own tag order first; remaining tags alphabetical; targets listed in ascending alias order (e.g., |001|002|…).

Idempotency & edge cases:

- If a note has no tags or no overlaps, it still adds a managed section with "(no related tags found)".
- Prior ## Tags (obsidian) is removed and rebuilt to guarantee idempotency.

Provides a human-friendly semantic map of your corpus mirroring the tag graph—excellent for discovery and cross-navigation in Obsidian.

2.1.7.15 015_references_linking.py — Build "## References (obsidian)" backlinks by DOI/Title

Purpose:
For each note, scans its References section and link entries to other notes in your vault using DOI first and title as fallback. Render a managed block such as:

References (obsidian)

- 3 [[Paper-X|001]]

- 7 [[Paper-Y|001]]

where numbers correspond to the original reference numbering.

Inputs/Outputs:

- Input: Two corpus indices built in a first pass:
    1. doi → filename (from Metadata ### DOI: and the fenced BibTeX block).
    2. normalized h1 title → filename.
- Output: Mirrored copies with a managed ## References (obsidian) appended to EOF (after removing any prior managed block).

Core logic:

- Same DOI/title extractors used by your DOI pipeline; reliable multi-line reference packing.
- Title normalization + fuzzy match (threshold tuned high to avoid false positives).
- Ignore self-links (a note won't point to itself).

Idempotency & edge cases:

- If a note lacks a references section or no matches are found, it adds a block with "(no reference links found)".
- Rebuilds the managed section cleanly on reruns.

Transforms the passive bibliography into active navigational backlinks within the vault—powered by DOIs/titles already curated.

2.1.7.16 Qualities across the pipeline

- **Idempotent/stable by design:** Normalizers (001, 003–006, 008, 009, 010, 014, 015) remove their own managed sections and rebuild them; reruns won't churn files.
- Safety rails:
  - Preserve YAML front-matter; keep originals; mirror to out-roots.
  - Avoid touching code fences (011 masks them before edits).
  - Section detection is tolerant (case/colons) yet uses strict boundaries (e.g., 010 requires ## Metadata to fence).
  - Dataset/tag scanners exclude References.
- **Strong regex discipline:** Multiline reference packing; robust header detection; title extraction that skips URLs/DOIs; exact DOI canonicalization.
- **Corpus-aware passes:** Keywords/tags (009) and Obsidian linkers (014–015) index the whole corpus first, then write file-local sections.
- Auditability:
  - Satellites/datasets → JSON/CSV;
  - Links → status CSV;
  - DOIs → audit CSV + JSON **cache** (fast reruns).
- Placement guarantees:
  - ## Linking appears between BibTeX and Metadata;
  - ### Datasets parsed: appears immediately after ### Dataset Used:;
  - BibTeX content is fenced only in the intended region;
  - Obsidian sections (## Tags (obsidian), ## References (obsidian)) are appended cleanly at EOF after removing prior managed versions.

2.2 Data Sources and Tables

2.2.1 Table of Satellites

Sensor / Satellite	Type	Bands / Resolution	Link	References
GeoEye-1	Optical	Panchromatic (41 cm), 4-band MS (1.65 m)	https://resources.maxar.com/data-sheets/geoeye-1	(Kholoshyn et al. 2023)
Landsat series (Landsat 5/8)	Optical	Landsat 5: 7 bands (30 m MS), 120 m thermal; Landsat 8: 11 bands (15–100 m)	https://earth.esa.int/eogateway/missions/landsat	(Kholoshyn et al. 2023)
MODIS (Terra/Aqua)	Optical	36 bands, 250 m–1 km	https://terra.nasa.gov/data/modis-data	(Kholoshyn et al. 2023)
Pléiades	Optical	Panchromatic (50 cm), 4-band MS (2 m)	https://earth.esa.int/eogateway/missions/pleiades	(Qing et al. 2022; Zhao and Zhang 2020)
QuickBird	Optical	Panchromatic (61 cm), 4-band MS (2.44 m)	https://earth.esa.int/eogateway/catalog/quickbird-full-archive	(Ji et al. 2018)
Sentinel-2	Optical	13 bands (VNIR/SWIR), 10–60 m	Sentinel-2 Info	(Butenko and Petrychenko 2023; Zitzlsberger et al. 2021; Ghorbanian et al. 2022; Ahmad et al. 2024)
SPOT 6/7	Optical	Panchromatic (1.5 m), 4-band MS (6 m)	https://earth.esa.int/eogateway/catalog/spot-6-and-7-esa-archive	(Cheng et al. 2021)
VIIRS (NOAA)	Optical	22 bands, 375 m (I-bands), 750 m (M-bands)	https://ncc.nesdis.noaa.gov/NOAA-21/index.php	(Ahmad et al. 2024)
WorldView-1/2/3 (DigitalGlobe/Maxar)	Optical	Panchromatic (31 cm), 8-band MS, SWIR, CAVIS	Maxar	(Tilon et al. 2020; Xia et al. 2023)

		(WorldView-3), varies by sensor		
ERS-1/2	SAR	C-band, 30 m (SAR)	https://earth.esa.int/eogateway/catalog/ers-1-2-sar-im-precision-l1-sar_imp_1p-	(Zitzlsberger et al. 2021)
Sentinel-1	SAR	C-band, dual polarization, 10 m+	Sentinel-1 Info	(Rao et al. 2023; Zitzlsberger et al. 2021; Boloorani et al. 2021; Dietrich et al. 2025)
TerraSAR-X	SAR	X-band, up to 1 m (VHR SAR)	TerraSAR-X	(Gong et al. 2016)
Envisat (ASAR)	SAR	C-band SAR, ~30 m (various modes)	https://earth.esa.int/eogateway/missions/envisat/asar	(Meyer 2019)
ALOS-1 PALSAR	SAR	L-band SAR, 10–100 m (Fine/ScanSAR)	https://www.eorc.jaxa.jp/ALOS/en/about/palsar.htm	(Gamba et al. 2007; Shimada et al. 2016)
ALOS-2 PALSAR-2	SAR	L-band SAR, ~3–10 m (Spotlight/Strip/Scan)	https://global.jaxa.jp/projects/sat/alos2/	(Yun et al. 2015; Shimada et al. 2016)
RADARSAT-1/2	SAR	C-band SAR, multi-mode	https://www.asc-csa.gc.ca/eng/satellites/radarsat2/	(Meyer 2019)
RCM (RADARSAT Constellation)	SAR	C-band SAR, ~3 satellites, ~3–100 m	https://www.asc-csa.gc.ca/eng/satellites/rcm/	(Meyer 2019)
COSMO-SkyMed	SAR	X-band SAR, up to ~1 m	https://www.asi.it/en/earth-science/cosmo-skymed/	(Yun et al. 2015)
PAZ	SAR	X-band SAR, up to ~1 m	https://www.inta.es/EN/PAZ-satellite/	(Meyer 2019)
SAOCOM 1A/1B	SAR	L-band SAR, ~10 m	https://www.conae.gov.ar/saocom	(Meyer 2019)

TanDEM-X	SAR	X-band (bi-static with TerraSAR-X)	https://www.dlr.de/en/tdmx	(Flores et al. 2019)

Tabelle 2: Satellites with type, bands and resolution, links and most important references

2.2.2 Table of Datasets and Data Sources

Name	Type	Description	Links
BigEarthNet	Benchmark Dataset	BigEarthNet v2.0 is a benchmark dataset consisting of 549,488 pairs of Sentinel-1 and Sentinel-2 image patches	https://bigearth.net/
ISPRS Vaihingen	Benchmark Dataset	High-resolution IR-R-G true orthophotos over Vaihingen, Germany (≈ 9 cm GSD) with accompanying DSM/nDSM and pixel-level ground-truth for urban 2D semantic labeling. Standard task defines six classes (impervious surfaces, buildings, low vegetation, trees, cars, clutter/background). Widely used to benchmark segmentation/feature-extraction methods for urban mapping and building/roof detection.	https://www.isprs.org/resources/datasets/benchmarks/UrbanSemLab/2d-sem-label-vaihingen.aspx
LEVIR-CD	Benchmark Dataset	Bi-temporal, high-resolution RGB imagery for building change detection, consisting of 637 co-registered image pairs (each 1024×1024 px, ≈0.5–0.8 m GSD) collected from multiple cities. Provides pixel-level change masks (~31k building-change instances) and standard train/val/test splits; widely used to benchmark deep learning methods for remote-sensing change detection.	https://justchenhao.github.io/LEVIR/
xBD Dataset / xView2	Benchmark Dataset	Large open-source dataset for building damage assessment from pre/post disaster satellite imagery (incl. polygons).	https://xview2.org/data
Copernicus Data Space Ecosystem	Data Repository	ESA's portal for free Sentinel-1 (SAR) and Sentinel-2 (optical) satellite imagery.	https://dataspace.copernicus.eu/
DeepGlobe Challenge (2018)	Data Repository	Datasets and code for satellite image road, building, and land cover segmentation (challenge archive).	http://deepglobe.org/challenge.html
Google Earth Engine Datasets	Data Repository	Access to global public geospatial datasets including Landsat, Sentinel, MODIS, and derived indices.	https://earthengine.google.com/datasets/
Inria Aerial Image Labeling Dataset	Data Repository	High-resolution orthorectified urban images with building mask labels, suitable for ML model training.	https://project.inria.fr/aerialimagelabeling/
Maxar Open Data Program	Data Repository	Public release of high-resolution pre/post-disaster satellite images for specific humanitarian events.	https://www.maxar.com/open-data
Microsoft Building Footprints	Data Repository	Precise, automatically extracted building footprints for much of the world.	https://github.com/microsoft/GlobalMLBuildingFootprints
OpenStreet Map (OSM)	Data Repository	Open global crowd-sourced vector database for building footprints, roads, and infrastructure.	https://www.openstreetmap.org/
Sentinel Hub	Data Repository	Streamlined browser-based and API-powered access to Sentinel, Landsat, and other sensors for rapid image retrieval.	https://www.sentinel-hub.com/

SpaceNet	Data Repository	Open satellite imagery and labeled building footprint datasets for urban mapping and ML training.	https://spacenet.ai/datasets/
Tomnod	Data Repository	Crowdsourced labeling platform for rapid mapping/disaster events (events as available; archive access varies). Discontinued 2019!	https://www.tomnod.com/
UNITAR / UNOSAT	Data Repository	Geospatial maps, damage assessments, and disaster/conflict event polygons produced by the United Nations.	https://unitar.org/maps
World Settlement Footprint (WSF)	Data Repository	Global raster dataset of built-up areas derived from Sentinel-1/2 by DLR.	https://www.dlr.de/eoc/en/desktopdefault.aspx/tabid-9628/16557_read-40454/
Dynamic World	Dataset	Global, near–real-time 10 m land-cover product derived from Sentinel-2 imagery, providing nine classes with per-pixel class probabilities and continuous temporal updates (2016→present). Accessible via Google Earth Engine and the Dynamic World app, it's commonly used for change detection, baseline masks, and training labels in remote sensing/ML workflows.	https://dynamicworld.app/
WorldCover	Dataset	The ESA WorldCover dataset provides a global land cover map at 10 m resolution derived from Sentinel-1 (SAR) and Sentinel-2 (optical) data. It delivers annual updates (2020, 2021, 2023) with 11 land cover classes following UN FAO LCCS standards. Designed for environmental monitoring, climate modelling, biodiversity assessment, agriculture, and urban studies, WorldCover offers free and	https://esa-worldcover.org/en

Tabelle 3: Datasets and Data Sources with links referenced in Literature

2.2.3 List of Datasets and Data Repositories

2.2.3.1 Open-source & benchmark Datasets

- xBD / xView2 (building damage, bitemporal VHR)
  Large-scale benchmark for post-disaster building damage with pre/post VHR imagery and polygon labels with ordinal damage levels; widely used for segmentation and damage classification baselines and transfer learning. Coverage spans multiple disasters and countries; still limited EU-specific morphology.
- SpaceNet (urban footprints & roads, VHR)
  Multi-round challenge datasets (e.g., building footprints, road extraction) with precise labels; geographic variety and consistent tiling.
- LEVIR-CD / LEVIR-CD+ (binary building change detection, bitemporal RGB)
  637+ co-registered image pairs (≈0.5–0.8 m GSD, 1024×1024) with pixel-level change masks and standard splits; widely used to benchmark CNN and transformer-based change detection.
- ISPRS Vaihingen / Potsdam (2D semantic labeling, aerial)
  High-resolution IR-R-G orthophotos (≈9 cm Vaihingen; 5–10 cm Potsdam) with DSM/nDSM and pixel-accurate ground truth for urban semantic segmentation (impervious, building, low veg, tree, car, clutter).
- Inria Aerial Image Labeling (aerial building masks)
  Orthorectified high-res urban imagery with building mask labels across multiple cities.
- DeepGlobe (2018, multi-task)
  Challenge datasets for road/building/land cover segmentation from satellite imagery.
- DOTA (Dataset for Object Detection in Aerial Images) – large-scale oriented object detection dataset (~15 categories, 280k instances, multiple sensors).
- LoveDA – land-cover dataset with urban/rural splits (2,500 Sentinel-2–based labeled images; widely used in semantic segmentation).
- WHU Building Dataset – 220k building footprints (30 cm aerial), used extensively for building extraction.

2.2.3.2 Humanitarian/operational datasets

- Copernicus Emergency Management Service (EMS)
  European rapid mapping for multiple events (flood, quake, conflict), providing AOI selections and vector products; useful for label transfer and validation in European contexts.
- UNITAR / UNOSAT
  Damage assessments and conflict/disaster mapping products (polygons/points) from expert and crowd-augmented analyses.
- Maxar Open Data Program (event VHR)
  Public release of pre/post VHR imagery for specific disasters/conflicts.
- ARIA Damage Proxy Map (DPM)
- Rapid InSAR coherence–based damage proxy layers for major events.
- OpenStreetMap (HOT OSM): humanitarian mapping campaigns providing rapid building footprints and road edits post-disaster.
- World Settlement Footprint (WSF) & Global Human Settlement Layer (GHSL): not per-event, but used operationally as baselines for exposure mapping.

2.2.3.3 Access portals / platform catalogs

- Copernicus Open Access Hub (SciHub, legacy)
  Free access to Sentinel-1 (SAR) and Sentinel-2 (optical). Note: phased out since 2023 and replaced by the Copernicus Data Space Ecosystem.
  https://scihub.copernicus.eu/
- Copernicus Data Space Ecosystem (CDSE, replacement)
  Successor to SciHub, providing free and open access to the full Sentinel archive (Sentinel-1/2/3/5P)

with scalable cloud storage and compute services.
https://dataspace.copernicus.eu/

- Sentinel Hub (API/tiling)
  API-based access and tiling for Sentinel, Landsat, and other sensors, including EO Browser for visualization.
  https://www.sentinel-hub.com/
- Google Earth Engine (GEE)
  Catalog of global geospatial datasets (Sentinel, Landsat, MODIS, VIIRS, DEMs, indices) with a scalable cloud analysis environment.
  https://earthengine.google.com/
- Maxar / Planet / other commercial portals
  Commercial portals for VHR tasking and archives (Maxar SecureWatch, Planet Explorer, Airbus OneAtlas, BlackSky, ICEYE, Capella, etc.); licensing applies.
- SkyFi
  Commercial marketplace and aggregator providing AOI selection, instant pricing, and ordering of archive imagery or new tasking. Aggregates access to multiple providers (optical and SAR, often VHR ≤30–50 cm; some also provide thermal/nighttime products).
  https://www.skyfi.com/
- UP42 (Airbus Defence & Space) – Aggregator platform combining data access (Pléiades, SPOT, Radar, and third-party sources) with hosted processing and analytics. https://up42.com/
- SkyWatch EarthCache – Aggregator for simplified access to multiple commercial constellations (optical, SAR, VHR), with transparent pricing and APIs for developers. https://skywatch.com/

2.2.3.4 Crowdsourced / community layers

- OpenStreetMap (OSM)
  Globally available footprints/roads (OSM
- Microsoft Building Footprints
  Globally available footprints and roads from community edits (OSM) and automatically extracted building footprints from VHR imagery (Microsoft, >1B buildings).
- Tomnod (archival)
  Historic crowdsourced labeling campaigns for disasters, discontinued in 2019; archival data remain available for selected events.

2.2.3.5 Global land-cover / settlement / elevation (context, masking, features)

- ESA WorldCover (10 m, annual)
  Global 10 m land-cover product derived from Sentinel-1 and Sentinel-2 with 11 classes; annual releases available for 2020, 2021, and 2023.
- Dynamic World (10 m, near-real-time)
  Global land-cover dataset derived from Sentinel-2 providing per-pixel class probabilities; continuously updated since 2016 and accessible via Google Earth Engine.
- World Settlement Footprint (WSF)
  Global built-up area maps at 10 m resolution produced by DLR from Sentinel-1/2 time series; editions released for 2015, 2019, and 2020.
- SRTM / Copernicus DEM / ALOS World 3D (AW3D30)
  Global digital elevation models providing near-global coverage at 30 m (SRTM), consistent DEMs at 30 m and 90 m (Copernicus DEM), and PRISM-based stereo elevation data at 30 m (ALOS AW3D30).

2.2.4 Table of Indices for Urban AOI Classification

Index / Metric	Type	Formula (spectral names)	Formula for Sentinel-2	Primary use in urban mask	Thresholding tips	Notes
NDVI (Normalized Difference Vegetation Index)	Optical	(NIR − Red) / (NIR + Red)	(B8 − B4) / (B8 + B4)	Suppress vegetation by excluding high-NDVI pixels	Scene-adaptive thresholds (e.g., Otsu or quantiles per AOI); urban candidates typically exhibit low NDVI (≈ <0.2–0.3 in many European cities/seasons, adjust per scene)	Standard for vegetation masking; reduces inclusion of parks/trees and false positives from vegetated roofs/medians (consistent with urban mapping practice in El Mendili et al., and spectral guidance in Bioucas-Dias et al.)
NDWI (Normalized Difference Water Index, McFeeters)	Optical	(Green − NIR) / (Green + NIR)	(B3 − B8) / (B3 + B8)	Suppress open water	Scene-adaptive masking of high NDWI values representing water bodies	Sensitive to NIR; deep building shadows may be misclassified as water—MNDWI often preferred in urban scenes
MNDWI (Modifie	Optical	(Green − SWIR) /	(B3 − B11) / (B3 + B11)	Suppress open water with	Otsu/quantiles per AOI to mask high MNDWI;	SWIR substitution increases

d NDWI, Xu)		(Green + SWIR)		improved robustness in urban areas	tune per illumination/season	water–impervious contrast; widely reported as more robust than NDWI in built-up contexts
NDBI (Normalized Difference Built-up Index)	Optical	(SWIR − NIR) / (SWIR + NIR)	(B11 – B8) / (B11 + B8)	Enhance impervious/ built-up surfaces	Retain higher NDBI as built-up cue; threshold varies with city/season and surface moisture	Simple and effective baseline cue for built-up detection; works best in combination with NDVI/MNDWI masks to suppress vegetation/water (urban usage consistent with El Mendili et al.)
IBI (Index-based Built-up Index)	Optical (composite)	Composite of normalized NDBI, NDVI, and MNDWI (IBI increases where NDBI is high and both NDVI and	Composite of NDBI, NDVI, MNDWI (normalized and combined)	Stabilize built-up detection by suppressing vegetation and water while enhancing impervious	Apply after vegetation and water masking; retain higher IBI as built-up candidates	More robust than NDBI alone in peri-urban and seasonally variable scenes; exact normalization follows published IBI formulations (Xu-type variants)

		MNDWI are low)				
VV/VH backscatter ratio (Sentinel-1)	SAR	VV ÷ VH	Ratio of S1 VV / VH	Confirm built-up areas via structural (double-bounce) response	Set scene-adaptive minimum ratio after radiometric terrain correction; evaluate distributions within AOI	Combine with amplitude masks; exclude layover/shadow in steep terrain; aligns with SAR operational guidance (Meyer; Plank)
Coherence (multi-temporal SLC, Sentinel-1)	SAR	Interferometric coherence across dates	Interferometric coherence across dates	Provide a stability prior for urban fabric	Retain pixels above a minimum coherence (scene-specific) to distinguish persistent man-made surfaces from decorrelating vegetation/agriculture	Helps through clouds/night; avoid vegetated/agricult

Tabelle 4: Indices for Urban Area AOI Classification (El Mendili et al. 2020; Meyer 2019; Plank 2014; Bioucas-Dias et al. 2013; Al-Khudhairy et al. 2005)

2.2.5 Table of ML Models used

Model Category	ML Model / Method	Paper Titles
Ensemble Learning	UISEM (RF, AdaBoost, GB, XGBoost)	(Ahmad et al. 2024)
	Random Forest	(Dietrich et al. 2025)
	Soft Voting Ensemble (XGBoost, etc.)	Building Disaster Detection from Satellite Images in War Zones Using Scalable Machine Learning
	CNN + Random Forest (Hybrid)	Measuring destruction from satellite images using deep-learning: Syrian Civil War
Neural Networks (ANN, DNN)	Artificial Neural Networks (ANN)	Application of Artificial Neural Networks for Mangrove Mapping Using Multi-Temporal and Multi-Source Remote Sensing Imagery
	Custom CNN	Building damage annotation on post-hurricane satellite imagery based on convolutional neural networks
	CNN (standard, flat)	Assessment of military destruction in Ukraine and its consequences using remote sensing
	CNN + RNN + GAN (GeoAI review)	GeoAI review on post-disaster building damage assessment with multisource remote sensing & social media
	BDD-Net (CNN, pixel-wise)	BDD-Net: A two-step deep learning model for multi-disaster building damage segmentation and classification using satellite imagery
U-Net Variants	BDANet (U-Net + ResNet + MFF + Attention)	A Deep Learning Application for Building Damage Assessment Using Ultra-High-Resolution Remote Sensing Imagery in Turkey Earthquake
	AU-Net (Attention U-Net)	Building Damage Detection in Satellite Imagery Using Convolutional Neural Networks (Wu et al., 2021)
	Siamese-U-Net (with attention)	Siamese U-Net: Dual-input architecture for fine-grained damage assessment (xBD)
	Dual-Stage U-Net	Building damage detection from satellite images after natural disasters on extremely imbalanced datasets
	EfficientNet U-Net	Fully convolutional Siamese neural networks for building damage assessment from satellite images (ISPRS Archives)
	BD-SKUNet (Selective Kernel UNet)	BD-SKUNet: Selective-Kernel UNets for Building Damage Assessment in High-Resolution Satellite Images
Siamese Networks	Siamese CNN + Attention	Building Damage Evaluation from Satellite Imagery using Deep Learning
	Siamese CNN (ResNet50-trained)	Assessing Building Damage by Learning the Deep Feature Correspondence of Before and After Aerial Images
	Siamese with EfficientNet & binary fusion	Siamese CNN-based architecture for xBD dataset (ISPRS 2022, EfficientNet B0/B5)
Transformer-based Models	SegDetector (SegFormer-based)	SegDetector: A transformer-based model for multi-temporal damage segmentation

	Multi-level Feature Guided Aggregation (CNN + Transformer)	Application of Remote Sensing Image Change Detection Algorithm in Extracting Damaged Buildings in Earthquake Disaster
	DAHITrA (Hierarchical Transformer)	Deep Neural Networks for Quantitative Damage Evaluation in Oblique UAV Images
	U-Net + Swin Transformer (Vision Transformer)	Generalizability of deep learning models for post-disaster building damage mapping
YOLO and Object Detection	SOCA-YOLO (YOLOv8 + Haar + Coord Attention)	SOCA-YOLO: Detecting War-Damaged Buildings Using Deep Learning and Satellite Imagery
Other Hybrid Models	BDANet (also includes multiscale feature fusion & CDA modules)	(Same as under U-Net Variants above — included here for completeness across categories)
	CC, PO, TTC, TTS (custom AlexNet-based CNNs)	Building Damage Detection in Satellite Imagery Using Convolutional Neural Networks (xBD baseline extension)
	Three-Stream CNN (VGG-based + binary masks)	Building Damage Assessment Using Deep Learning and Ground-Level Image Data (Rashedi et al., 2017)
	U-Net + ResNet/SEResNeXt/SENet/DualPathNet	Transferable CNNs for war damage detection on VHR imagery (Mariupol Study)

Tabelle 5: ML Models by Category

2.3 Glossary and Definitions

Heterogeneity Characteristics

Heterogeneity Characteristics of Damaged Buildings Damaged structures exhibit complex and diverse traits in terms of spectral information, texture, morphology, and context, reflecting high variability in how they appear and are detected(Y. Xie et al. 2022).

Remote Sensing Technologies

Remote Sensing is the technique of using satellite imagery and aerial data to observe and study the Earth's surface without making physical contact. (Bonchkovskyi et al. 2023)

SAR

Synthetic Aperture Radar (SAR) A radar-based imaging system that sends and receives pulses continuously from a moving platform (like a satellite or airplane), enabling high-resolution mapping. (Rao et al. 2023)

Image Feature Extraction & Vision Models

Deep Features High-level representations extracted from images using Convolutional Neural Networks (CNNs), capturing deeper semantic information beyond basic pixel values. (Presa-Reyes and Chen 2020)

Swin Transformer

A transformer-based vision model that applies attention mechanisms to achieve powerful image understanding, often outperforming traditional CNNs in complex tasks.(Cui et al. 2023)

2.4 Acronyms and Abbreviations

Acronym / Abbreviation	Short Description or Full Term
ANN	Artificial Neural Network
AOI	Area of Interest
ARIA	Advanced Rapid Imaging and Analysis (InSAR product by NASA/JPL)
AU-Net	Attention U-Net (U-Net with attention mechanism)
BDANet	Building Damage Assessment Network (deep learning model)
BDD-Net	Building Damage Detection Network (CNN for damage segmentation)
BoVW	Bag of Visual Words (image feature extraction method)
CC	Concatenated Channel model (in change detection/CNNs)
CBAM	Convolutional Block Attention Module (attention in deep networks)
CDA	Cross-Directional Attention (feature fusion module)
CNN	Convolutional Neural Network
Coherence	SAR signal stability metric (change detection in SAR imagery)
DPM	Damage Proxy Map (SAR-based change detection product)
DSM	Digital Surface Model
DS	Depthwise Separable (as in depthwise separable convolution)
DualPathNet	Dual Path Network (CNN encoder variant)
DRS	Deep Recurrent Sensor(s) (context: multi-temporal network)
ECA	Efficient Channel Attention (CNN attention mechanism)
EMS-98	European Macroseismic Scale 1998 (building damage/classification scale)
EO	Earth Observation
ERCNN-DRS	Ensemble of Recurrent Convolutional Neural Networks for Disaster Response System
ESA	European Space Agency
FPN	Feature Pyramid Network (deep learning decoder/structure)

GAN	Generative Adversarial Network
GDAL	Geospatial Data Abstraction Library (open-source geospatial data library)
GIS	Geographic Information System
GLCM	Gray-Level Co-occurrence Matrix (texture feature extraction)
HRNet	High-Resolution Network (deep learning architecture for segmentation)
HPO	Hyperparameter Optimization
IDA	Ida Dataset (damage dataset; or, in general, 'Index Data Access' if out of context)
IoU	Intersection over Union (metric for segmentation accuracy)
InSAR	Interferometric Synthetic Aperture Radar
KNN	K-Nearest Neighbors (machine learning classifier)
LDA	Latent Dirichlet Allocation (topic modeling / clustering technique)
LSTM	Long Short-Term Memory (recurrent neural network)
mAP	Mean Average Precision (metric for detection/classification)
MFF	Multiscale Feature Fusion
ML	Machine Learning
MODIS	Moderate Resolution Imaging Spectroradiometer
MS	Multispectral (descriptor for satellite data/hypercube)
NDBI	Normalized Difference Built-Up Index (satellite-derived urban index)
NDVI	Normalized Difference Vegetation Index
NMS	Non-Maximum Suppression (post-processing in detection models)
OA	Overall Accuracy
OBIA	Object-Based Image Analysis
OSM	OpenStreetMap
PALSAR	Phased Array L-band Synthetic Aperture Radar
PGA	Peak Ground Acceleration (seismic hazard parameter)
PO	Post Only (in the context of CNN post-damage stream)
PSPNet	Pyramid Scene Parsing Network (semantic segmentation CNN)

QGIS	Quantum GIS (open-source GIS application)
R-CNN	Region-based Convolutional Neural Network
RAISE	Rapid Assessment of Infrastructure using Satellite and aerial Earth observation data (may also appear as "RAISE" project)
ResNet	Residual Neural Network (deep CNN architecture)
RF	Random Forest (machine learning ensemble method)
ROI	Region of Interest
SAR	Synthetic Aperture Radar
SBAS	Small Baseline Subset (method in InSAR timeseries processing)
SIFT	Scale-Invariant Feature Transform (image descriptor)
SLC	Single-Look Complex (SAR data format)
SVM	Support Vector Machine
SWIR	Short-Wave Infrared (spectral region, 1–2.5 µm)
TTS	Twin-Tower Subtract model (CNN variant for change detection)
UAV	Unmanned Aerial Vehicle (drone imagery)
U-Net	U-shaped deep learning network for image segmentation
UISEM	Urban Impervious Surface Extraction Model (ensemble ML for urban mapping)
UNOSAT	United Nations Operational Satellite Applications Programme
VGG	Visual Geometry Group Net (deep CNN architecture)
ViT	Vision Transformer (transformer-based model for vision)
VHR	Very High Resolution (image spatial resolution <1m–2m)
WMS	Web Map Service (OGC standard)
WFS	Web Feature Service (OGC standard)
xBD	Extreme Building Damage Dataset (large open post-disaster satellite image dataset)

Tabelle 6: Acronyms and Abbreviations

2.5 List of Images

2.6 List of Tables

2.7 References

Adams, John B., Milton O. Smith, and Paul E. Johnson. 1986. “Spectral Mixture Modeling: A New Analysis of Rock and Soil Types at the Viking Lander 1 Site.” *Journal of Geophysical Research: Solid Earth* 91 (B8): 8098–112. https://doi.org/10.1029/JB091iB08p08098.

Adriano, Bruno, Naoto Yokoya, Junshi Xia, et al. 2021. “Learning from Multimodal and Multitemporal Earth Observation Data for Building Damage Mapping.” *ISPRS Journal of Photogrammetry and Remote Sensing* 175: 132–43. https://doi.org/10.1016/j.isprsjprs.2021.02.016.

Ahmad, Muhammad Nasar, Zhenfeng Shao, Xiongwu Xiao, Peng Fu, Akib Javed, and Iffat Ara. 2024. “A Novel Ensemble Learning Approach to Extract Urban Impervious Surface Based on Machine Learning Algorithms Using SAR and Optical Data.” *International Journal of Applied Earth Observation and Geoinformation* 132 (August): 104013. https://doi.org/10.1016/j.jag.2024.104013.

Ahmadi, Seyed Ali, Ali Mohammadzadeh, Naoto Yokoya, and Arsalan Ghorbanian. 2023. “BD-SKUNet: Selective-Kernel UNets for Building Damage Assessment in High-Resolution Satellite Images.” *Remote Sensing* 16 (1): 182. https://doi.org/10.3390/rs16010182.

Aimaiti, Yusupujiang, Christina Sanon, Magaly Koch, Laurie G. Baise, and Babak Moaveni. 2022. “War Related Building Damage Assessment in Kyiv, Ukraine, Using Sentinel-1 Radar and Sentinel-2 Optical Images.” *Remote Sensing* 14 (24): 6239. https://doi.org/10.3390/rs14246239.

Al Shafian, Sultan, Chao He, and Da Hu. 2025. “DamageScope: An Integrated Pipeline for Building Damage Segmentation, Geospatial Mapping, and Interactive Web-Based Visualization.” *Remote Sensing* 17 (13): 2267. https://doi.org/10.3390/rs17132267.

Al-Khudhairy, D.H.A., I. Caravaggi, and S. Giada. 2005. “Structural Damage Assessments from Ikonos Data Using Change Detection, Object-Oriented Segmentation, and Classification Techniques.” *Photogramm Eng Remote Sensing* 71 (7): 7. https://doi.org/10.14358/PERS.71.7.825.

Alphonse, Abhishek Bamby, Tomasz Wawrzyniak, Marzena Osuch, and Nicole Hanselmann. 2023. “Applying UAV-Based Remote Sensing Observation Products in High Arctic Catchments in SW Spitsbergen.” *Remote Sensing* 15 (4): 934. https://doi.org/10.3390/rs15040934.

Andress, Jason. 2014. *Cyber Warfare: Techniques, Tactics and Tools for Security Practitioners*. 2nd ed. With Steve Winterfeld. Syngress.

Antoniou, Antreas, Amos Storkey, and Harrison Edwards. 2018. “Data Augmentation Generative Adversarial Networks.” arXiv:1711.04340. Preprint, arXiv, March 21. https://doi.org/10.48550/arXiv.1711.04340.

Armed Conflict in the East of Ukraine: The Damage Caused to the Housing of the Civilian Population = Zbrojnyj Konflikt Na Schodi Ukraïny : Škoda, Zavdana Žytlu Cyvil’noho Naselennja. 2019. With Мельник, Наталія М. Human Rights Publisher.

Ayush, Kumar, Burak Uzkent, Chenlin Meng, et al. 2021. “Geography-Aware Self-Supervised Learning.” *2021 IEEE/CVF International Conference on Computer Vision (ICCV)*, October, 10161–70. https://doi.org/10.1109/ICCV48922.2021.01002.

Badrinarayanan, Vijay, Alex Kendall, and Roberto Cipolla. 2017. “SegNet: A Deep Convolutional Encoder-Decoder Architecture for Image Segmentation.” *IEEE Transactions on Pattern Analysis and Machine Intelligence* 39 (12): 2481–95. https://doi.org/10.1109/TPAMI.2016.2644615.

Balz, Timo, and Mingsheng Liao. 2010. “Building-Damage Detection Using Post-Seismic High-Resolution SAR Satellite Data.” *International Journal of Remote Sensing* 31 (13): 3369–91. https://doi.org/10.1080/01431161003727671.

“BaseMap - GEOINT | OSM.” n.d. Accessed July 31, 2025. https://osm.gs.mil/product/basemap.

“Battle Damage Assessment - an Overview | ScienceDirect Topics.” n.d. Accessed August 30, 2025. https://www.sciencedirect.com/topics/computer-science/battle-damage-assessment.

Benedetti, Paola, Dino Ienco, Raffaele Gaetano, Kenji Ose, Ruggero G. Pensa, and Stephane Dupuy. 2018. “Fusion: A Deep Learning Architecture for Multiscale Multimodal Multitemporal Satellite Data Fusion.” *IEEE Journal of Selected Topics in Applied Earth Observations and Remote Sensing* 11 (12): 4939–49. https://doi.org/10.1109/JSTARS.2018.2876357.

Benson, Vitus, and Alexander Ecker. 2020. “Assessing Out-of-Domain Generalization for Robust Building Damage Detection.” arXiv:2011.10328. Preprint, arXiv, November 20. https://doi.org/10.48550/arXiv.2011.10328.

Berger, Michael, Jose Moreno, Johnny A. Johannessen, Pieternel F. Levelt, and Ramon F. Hanssen. 2012. “ESA’s Sentinel Missions in Support of Earth System Science.” *Remote Sensing of Environment*, The Sentinel Missions - New Opportunities for Science, vol. 120 (May): 84–90. https://doi.org/10.1016/j.rse.2011.07.023.

Bhardwaj, Diwakar, N. Nagabhooshanam, Ajeet Singh, et al. 2025. *Enhanced Satellite Imagery Analysis for Post-Disaster Building Damage Assessment Using Integrated ResNet-U-Net Model*. 84 (5): 2689–714. https://doi.org/10.1007/s11042-024-20300-0.

Bioucas-Dias, Jose M., Antonio Plaza, Gustavo Camps-Valls, Paul Scheunders, Nasser Nasrabadi, and Jocelyn Chanussot. 2013. “Hyperspectral Remote Sensing Data Analysis and Future Challenges.” *IEEE Geoscience and Remote Sensing Magazine* 1 (2): 6–36. https://doi.org/10.1109/MGRS.2013.2244672.

Blaschke, T. 2010. “Object Based Image Analysis for Remote Sensing.” *ISPRS Journal of Photogrammetry and Remote Sensing* 65 (1): 2–16. https://doi.org/10.1016/j.isprsjprs.2009.06.004.

Blaschke, Thomas, Geoffrey J. Hay, Maggi Kelly, et al. 2014. “Geographic Object-Based Image Analysis – Towards a New Paradigm.” *ISPRS Journal of Photogrammetry and Remote Sensing* 87 (January): 180–91. https://doi.org/10.1016/j.isprsjprs.2013.09.014.

Boloorani, Ali Darvishi, Mehdi Darvishi, Qihao Weng, and Xiangtong Liu. 2021. “Post-War Urban Damage Mapping Using InSAR: The Case of Mosul City in Iraq.” *IJGI* 10 (3): 140. https://doi.org/10.3390/ijgi10030140.

Bonchkovskyi, Oleksandr S., Pavlo O. Ostapenko, Volodymyr M. Shvaiko, and Andrii S. Bonchkovskyi. 2023. “Remote Sensing as a Key Tool for Assessing War-Induced Damage to Soil Cover in Ukraine (the Case Study of Kyinska Territorial Hromada).” *Journal of Geology, Geography and Geoecology* 32 (3): 474–87. https://doi.org/10.15421/112342.

Bouchard, Isabelle, Marie-Ève Rancourt, Daniel Aloise, and Freddie Kalaitzis. 2022. “On Transfer Learning for Building Damage Assessment from Satellite Imagery in Emergency Contexts.” *Remote Sensing* 14 (11): 11. https://doi.org/10.3390/rs14112532.

Braik, Abdullah M., and Maria Koliou. 2024. “Automated Building Damage Assessment and Large-scale Mapping by Integrating Satellite Imagery, GIS, and Deep Learning.” *Computer Aided Civil Eng* 39 (15): 15. https://doi.org/10.1111/mice.13197.

Braun, Andreas. 2018. “Assessment of Building Damage in Raqqa during the Syrian Civil War Using Time-Series of Radar Satellite Imagery.” *GI_Forum* 1: 228–42. https://doi.org/10.1553/giscience2018_01_s228.

Breiman, Leo. 2001. “Random Forests.” *Machine Learning* 45 (1): 5–32. https://doi.org/10.1023/A:1010933404324.

Brown, Christopher F., Michal R. Kazmierski, Valerie J. Pasquarella, et al. 2025. “AlphaEarth Foundations: An Embedding Field Model for Accurate and Efficient Global Mapping from Sparse Label Data.” arXiv:2507.22291. Preprint, arXiv, July 29. https://doi.org/10.48550/arXiv.2507.22291.

Burnett, C, and Thomas Blaschke. 2003. “A Multi-Scale Segmentation/Object Relationship Modelling Methodology for Landscape Analysis.” *Ecological Modelling*, Landscape Theory and Landscape Modelling, vol. 168 (3): 233–49. https://doi.org/10.1016/S0304-3800(03)00139-X.

Butenko, Ye., and S. Petrychenko. 2023. “Monitoring and Assessment of the Scale of Destruction by Remote Sensing Methods During the War in Ukraine.” *International Conference of Young Professionals «GeoTerrace-2023»* (Lviv, Ukraine,), 1–5. https://doi.org/10.3997/2214-4609.2023510105.

Calantropio, A., F. Chiabrando, M. Codastefano, and E. Bourke. 2021. “DEEP LEARNING FOR AUTOMATIC BUILDING DAMAGE ASSESSMENT: APPLICATION IN POST-DISASTER SCENARIOS USING UAV DATA.” *ISPRS Ann. Photogramm. Remote Sens. Spatial Inf. Sci.* V-1–2021 (June): 113–20. https://doi.org/10.5194/isprs-annals-V-1-2021-113-2021.

Canny, John. 1986. “A Computational Approach to Edge Detection.” *IEEE Transactions on Pattern Analysis and Machine Intelligence* PAMI-8 (6): 679–98. https://doi.org/10.1109/TPAMI.1986.4767851.

Cao, Quoc Dung, and Youngjun Choe. 2020. “Building Damage Annotation on Post-Hurricane Satellite Imagery Based on Convolutional Neural Networks.” *Nat Hazards* 103 (3): 3. https://doi.org/10.1007/s11069-020-04133-2.

Cao, Quoc Dung, and Youngjun Choe. 2024. “Posthurricane Damage Assessment Using Satellite Imagery and Geolocation Features.” *Risk Analysis* 44 (5): 5. https://doi.org/10.1111/risa.14244.

Casana, Jesse, and Elise Jakoby Laugier. 2017. “Satellite Imagery-Based Monitoring of Archaeological Site Damage in the Syrian Civil War.” *PLoS ONE* 12 (11): 11. https://doi.org/10.1371/journal.pone.0188589.

Chawanji, Sharon, Kristin Fleischer, and Jörg Ullrich. 2022. “Copernicus Emergency Management Service (CEMS) – Risk and Recovery Mapping.” *Abstracts of the ICA* 5 (September): 1–2. https://doi.org/10.5194/ica-abs-5-118-2022.

Chen, Liang-Chieh, George Papandreou, Iasonas Kokkinos, Kevin Murphy, and Alan L. Yuille. 2017. “DeepLab: Semantic Image Segmentation with Deep Convolutional Nets, Atrous Convolution, and Fully Connected CRFs.” arXiv:1606.00915. Preprint, arXiv, May 12. https://doi.org/10.48550/arXiv.1606.00915.

Chen, Tao, Zhiyuan Lu, Yue Yang, Yuxiang Zhang, Bo Du, and Antonio Plaza. 2022. “A Siamese Network Based U-Net for Change Detection in High Resolution Remote Sensing Images.” *IEEE Journal of Selected Topics in Applied Earth Observations and Remote Sensing* 15: 2357–69. https://doi.org/10.1109/JSTARS.2022.3157648.

Chen, Ting, Simon Kornblith, Mohammad Norouzi, and Geoffrey Hinton. 2020. “A Simple Framework for Contrastive Learning of Visual Representations.” *Proceedings of the 37th International Conference on Machine Learning*, ICML’20, vol. 119 (July): 1597–607.

Cheng, Chih-Shen, Amir H. Behzadan, and Arash Noshadravan. 2021. “Deep Learning for Post-hurricane Aerial Damage Assessment of Buildings.” *Computer-Aided Civil and Infrastructure Engineering* 36 (6): 695–710. https://doi.org/10.1111/mice.12658.

Clark, Robert M. 2020. *Geospatial Intelligence: Origins and Evolution*. 1st ed. Georgetown University Press.

Clark, Roger N., Gregg A. Swayze, K. Eric Livo, et al. 2003. “Imaging Spectroscopy: Earth and Planetary Remote Sensing with the USGS Tetracorder and Expert Systems.” *Journal of Geophysical Research: Planets* 108 (E12). https://doi.org/10.1029/2002JE001847.

Congalton, Russell G. 1991. “A Review of Assessing the Accuracy of Classifications of Remotely Sensed Data.” *Remote Sensing of Environment* 37 (1): 35–46. https://doi.org/10.1016/0034-4257(91)90048-B.

Cortes, Corinna, and Vladimir Vapnik. 1995. “Support-Vector Networks.” *Machine Learning* 20 (3): 273–97. https://doi.org/10.1007/BF00994018.

Cui, Liangyi, Xin Jing, Yu Wang, Yixuan Huan, Yang Xu, and Qiangqiang Zhang. 2023. “Improved Swin Transformer-Based Semantic Segmentation of Postearthquake Dense Buildings in Urban Areas Using Remote Sensing Images.” *IEEE Journal of Selected Topics in Applied Earth Observations and Remote Sensing* 16: 369–85. https://doi.org/10.1109/JSTARS.2022.3225150.

Daudt, Rodrigo Caye, Bertrand Le Saux, and Alexandre Boulch. 2018. “Fully Convolutional Siamese Networks for Change Detection.” arXiv:1810.08462. Preprint, arXiv, October 19. https://doi.org/10.48550/arXiv.1810.08462.

“Defence | Airbus.” 2024. May 30. https://www.airbus.com/en/products-services/defence.

Dietrich, Olivier, Torben Peters, Vivien Sainte Fare Garnot, et al. 2025. “An Open-Source Tool for Mapping War Destruction at Scale in Ukraine Using Sentinel-1 Time Series.” *Commun Earth Environ* 6 (1): 1. https://doi.org/10.1038/s43247-025-02183-7.

Drusch, M., U. Del Bello, S. Carlier, et al. 2012. “Sentinel-2: ESA’s Optical High-Resolution Mission for GMES Operational Services.” *Remote Sensing of Environment*, The Sentinel Missions - New Opportunities for Science, vol. 120 (May): 25–36. https://doi.org/10.1016/j.rse.2011.11.026.

El Mendili, Lamiae, Anne Puissant, Mehdi Chougrad, and Imane Sebari. 2020. “Towards a Multi-Temporal Deep Learning Approach for Mapping Urban Fabric Using Sentinel 2 Images.” *Remote Sensing* 12 (3): 423. https://doi.org/10.3390/rs12030423.

Endo, Yukio, Bruno Adriano, Erick Mas, and Shunichi Koshimura. 2018. “New Insights into Multiclass Damage Classification of Tsunami-Induced Building Damage from SAR Images.” *Remote Sensing* 10 (12): 2059. https://doi.org/10.3390/rs10122059.

Etten, Adam, Dave Lindenbaum, and Todd Bacastow. 2018. *SpaceNet: A Remote Sensing Dataset and Challenge Series*. https://doi.org/10.48550/arXiv.1807.01232.

Etten, Adam Van, and Daniel Hogan. 2021. “The SpaceNet Multi-Temporal Urban Development Challenge.” arXiv:2102.11958. Preprint, arXiv, May 20. https://doi.org/10.48550/arXiv.2102.11958.

“European Union.” 2025. August 22. https://european-union.europa.eu/index_en.

Flores, Africa, K. Herndon, Rajesh Thapa, and Emil Cherrington. 2019. *Synthetic Aperture Radar (SAR) Handbook: Comprehensive Methodologies for Forest Monitoring and Biomass Estimation*. https://doi.org/10.25966/NR2C-S697.

Gamba, Paolo, Fabio Dell’Acqua, and Giovanna Trianni. 2007. “Rapid Damage Detection in the Bam Area Using Multitemporal SAR and Exploiting Ancillary Data.” *IEEE Transactions on Geoscience and Remote Sensing* 45 (6): 1582–89. https://doi.org/10.1109/TGRS.2006.885392.

Gao, Bo-Cai. 1996. “NDWI—A Normalized Difference Water Index for Remote Sensing of Vegetation Liquid Water from Space.” *Remote Sensing of Environment* 58 (3): 257–66.

Garzón, Fernando Arturo MENDEZ, and István Valánszki. 2020. “REMOTE SENSING TENDENCIES IN THE ASSESSMENT OF AREAS DAMAGED BY ARMED CONFLICTS.” *Earth Observation*.

German Aerospace Center. 2023. “World Settlement Footprint (WSF) 2019 - Sentinel-1/2 - Global.” German Aerospace Center (DLR). https://doi.org/10.15489/TWG5XSNQUW84.

Ghorbanian, Arsalan, Seyed Ali Ahmadi, Meisam Amani, Ali Mohammadzadeh, and Sadegh Jamali. 2022. “Application of Artificial Neural Networks for Mangrove Mapping Using Multi-Temporal and Multi-Source Remote Sensing Imagery.” *Water* 14 (2): 244. https://doi.org/10.3390/w14020244.

Gibril, Mohamed Barakat A., Rami Al-Ruzouq, Abdallah Shanableh, et al. 2024. “Transformer-Based Semantic Segmentation for Large-Scale Building Footprint Extraction from Very-High Resolution Satellite Images.” *Advances in Space Research* 73 (10): 4937–54. https://doi.org/10.1016/j.asr.2024.03.002.

Gong, Lixia, Chao Wang, Fan Wu, Jingfa Zhang, Hong Zhang, and Qiang Li. 2016. “Earthquake-Induced Building Damage Detection with Post-Event Sub-Meter VHR TerraSAR-X Staring Spotlight Imagery.” *Remote Sensing* 8 (11): 11. https://doi.org/10.3390/rs8110887.

Gonzalez, Rafael C., and Richard E. Woods. 2018. *Digital Image Processing*. Pearson.

Goodfellow, Ian, Yoshua Bengio, and Aaron Courville. 2016. *Deep Learning*. MIT Press.

Goodfellow, Ian, Jean Pouget-Abadie, Mehdi Mirza, et al. 2014. “Generative Adversarial Networks.” *Advances in Neural Information Processing Systems* 3 (June). https://doi.org/10.1145/3422622.

Gorelick, Noel, Matt Hancher, Mike Dixon, Simon Ilyushchenko, David Thau, and Rebecca Moore. 2017. “Google Earth Engine - Planetary-Scale Geospatial Analysis for Everyone.” *Remote Sensing of Environment*, Big Remotely Sensed Data: tools, applications and experiences, vol. 202 (December): 18–27. https://doi.org/10.1016/j.rse.2017.06.031.

Green, Robert O, Michael L Eastwood, Charles M Sarture, et al. 1998. “Imaging Spectroscopy and the Airborne Visible/Infrared Imaging Spectrometer (AVIRIS).” *Remote Sensing of Environment* 65 (3): 227–48. https://doi.org/10.1016/S0034-4257(98)00064-9.

Grill, Jean-Bastien, Florian Strub, Florent Altché, et al. 2020. “Bootstrap Your Own Latent a New Approach to Self-Supervised Learning.” *Proceedings of the 34th International Conference on Neural Information Processing Systems* (Red Hook, NY, USA), NIPS ’20, 21271–84.

Guanter, Luis, Hermann Kaufmann, Karl Segl, et al. 2015. “The EnMAP Spaceborne Imaging Spectroscopy Mission for Earth Observation.” *Remote Sensing* 7 (7): 8830–57. https://doi.org/10.3390/rs70708830.

Guo, Chuan, Geoff Pleiss, Yu Sun, and Kilian Q. Weinberger. 2017. “On Calibration of Modern Neural Networks.” *Proceedings of the 34th International Conference on Machine Learning*, July 17, 1321–30. https://proceedings.mlr.press/v70/guo17a.html.

Gupta, Neha, Shikha Chadha, Rosey Chauhan, and Pooja Singhal. 2024. “Damage Evaluation Following Natural Disasters Using Deep Learning.” In *Advanced Computing*, edited by Deepak Garg, Joel J. P. C. Rodrigues, Suneet Kumar Gupta, Xiaochun Cheng, Pushpender Sarao, and Govind Singh Patel. Springer Nature Switzerland. https://doi.org/10.1007/978-3-031-56703-2_8.

Gupta, Ritwik, Richard Hosfelt, Sandra Sajeev, et al. 2019. “xBD: A Dataset for Assessing Building Damage from Satellite Imagery.” arXiv:1911.09296. Preprint, arXiv, November 21. https://doi.org/10.48550/arXiv.1911.09296.

Gupta, Rohit, and Mubarak Shah. 2021. “RescueNet: Joint Building Segmentation and Damage Assessment from Satellite Imagery.” *2020 25th International Conference on Pattern Recognition (ICPR)* (Milan, Italy), January, 4405–11. https://doi.org/10.1109/ICPR48806.2021.9412295.

Hao, Hanxiang, Sriram Baireddy, Emily R. Bartusiak, et al. 2021. “An Attention-Based System for Damage Assessment Using Satellite Imagery.” *2021 IEEE International Geoscience and Remote Sensing Symposium IGARSS*, 4396–99. https://doi.org/10.1109/IGARSS47720.2021.9554054.

Hao, Xuejie, Lu Liu, Rongjin Yang, Lizeyan Yin, Le Zhang, and Xiuhong Li. 2023. “A Review of Data Augmentation Methods of Remote Sensing Image Target Recognition.” *Remote Sensing* 15 (3): 827. https://doi.org/10.3390/rs15030827.

He, Kaiming, Haoqi Fan, Yuxin Wu, Saining Xie, and Ross Girshick. 2020. “Momentum Contrast for Unsupervised Visual Representation Learning.” *2020 IEEE/CVF Conference on Computer Vision and Pattern Recognition (CVPR)*, June, 9726–35. https://doi.org/10.1109/CVPR42600.2020.00975.

He, Kaiming, Xiangyu Zhang, Shaoqing Ren, and Jian Sun. 2016. “Deep Residual Learning for Image Recognition.” *2016 IEEE Conference on Computer Vision and Pattern Recognition (CVPR)*, June, 770–78. https://doi.org/10.1109/CVPR.2016.90.

Heipke, Christian. 2010. “Crowdsourcing Geospatial Data.” *ISPRS Journal of Photogrammetry and Remote Sensing*, ISPRS Centenary Celebration Issue, vol. 65 (6): 550–57. https://doi.org/10.1016/j.isprsjprs.2010.06.005.

Herfort, Benjamin, Sven Lautenbach, João Porto de Albuquerque, Jennings Anderson, and Alexander Zipf. 2021. “The Evolution of Humanitarian Mapping within the OpenStreetMap Community.” *Scientific Reports* 11 (1): 3037. https://doi.org/10.1038/s41598-021-82404-z.

Hewawiththi, Nethmi S., M. Mahesha Viduranga, Vanodhya G. Warnasooriya, et al. 2024. “Damage Assessment after Natural Disasters with UAVs: Semantic Feature Extraction Using Deep Learning.” Preprint, arXiv. https://doi.org/10.48550/ARXIV.2412.10756.

Hinton, G. E., and R. R. Salakhutdinov. 2006. “Reducing the Dimensionality of Data with Neural Networks.” *Science* 313 (5786): 504–7. https://doi.org/10.1126/science.1127647.

Holail, Shimaa, Tamer Saleh, Xiongwu Xiao, et al. 2024. “Time-Series Satellite Remote Sensing Reveals Gradually Increasing War Damage in the Gaza Strip.” *National Science Review* 11 (9): 9. https://doi.org/10.1093/nsr/nwae304.

Hou, Yandong, Kaiwen Liu, Xiaodong Zhai, and Zhengquan Chen. 2024. “Mbda-Net: A Building Damage Assessment Model Based on a Multi-Scale Fusion Network.” *Signal, Image and Video Processing* 18 (12): 9363–74. https://doi.org/10.1007/s11760-024-03551-0.

Huang, Gao, Zhuang Liu, Laurens Van Der Maaten, and Kilian Q. Weinberger. 2017. “Densely Connected Convolutional Networks.” *2017 IEEE Conference on Computer Vision and Pattern Recognition (CVPR)*, July, 2261–69. https://doi.org/10.1109/CVPR.2017.243.

I. T. Jolliffe. 2002. *Principal Component Analysis*. Springer Series in Statistics. Springer-Verlag. https://doi.org/10.1007/b98835.

“ICRC.” 2025. https://www.icrc.org/en.

James B. Campbell and Randolph H. Wynne. 2011. *Introduction to Remote Sensing*. 5th ed. Vol. 5. Guilford Press, New York. https://www.mdpi.com/2072-4292/5/1/282.

Jensen, John R. 2016. *Introductory Digital Image Processing: A Remote Sensing Perspective*. 4th ed. Pearson Series in Geographic Information Science. Pearson Education.

Ji, Min, Lanfa Liu, and Manfred Buchroithner. 2018. "Identifying Collapsed Buildings Using Post-Earthquake Satellite Imagery and Convolutional Neural Networks: A Case Study of the 2010 Haiti Earthquake." *Remote Sensing* 10 (11): 1689. https://doi.org/10.3390/rs10111689.

Jolliffe, Ian T., and Jorge Cadima. 2016. "Principal Component Analysis: A Review and Recent Developments." *Philosophical Transactions of the Royal Society A: Mathematical, Physical and Engineering Sciences* 374 (2065): 20150202. https://doi.org/10.1098/rsta.2015.0202.

Joy-Fares, Arshad, Raja Rehan,Aoun. n.d. "Syria Damage Assessment of Selected Cities Aleppo, Hama, Idlib." Text/HTML. World Bank. Accessed August 30, 2025. https://documents.worldbank.org/en/publication/documents-reports/documentdetail/530541512657033401.

Kang, Dae Kun, Michael J. Olsen, Erica Fischer, and Jaehoon Jung. 2025. "Residential Wildfire Structural Damage Detection Using Deep Learning to Analyze Uncrewed Aerial System Imagery, Aerial Imagery, and Satellite Imagery." *Fire and Materials*, February, fam.3282. https://doi.org/10.1002/fam.3282.

Kerle, Norman, Francesco Nex, Markus Gerke, Diogo Duarte, and Anand Vetrivel. 2020. "UAV-Based Structural Damage Mapping: A Review." *ISPRS International Journal of Geo-Information* 9 (1): 14. https://doi.org/10.3390/ijgi9010014.

Kholoshyn, I V, M J Syvyj, S V Mantulenko, O L Shevchenko, D Sherick, and K M Mantulenko. 2023. "Assessment of Military Destruction in Ukraine and Its Consequences Using Remote Sensing." *IOP Conference Series: Earth and Environmental Science* 1254 (1): 012132. https://doi.org/10.1088/1755-1315/1254/1/012132.

Khvedchenya, Eugene, and Tatiana Gabruseva. 2021. "Fully Convolutional Siamese Neural Networks for Buildings Damage Assessment from Satellite Images." arXiv. https://doi.org/10.48550/ARXIV.2111.00508.

Kim, Taeheon, and Youkyung Han. 2021. "Integrated Preprocessing of Multitemporal Very-High-Resolution Satellite Images via Conjugate Points-Based Pseudo-Invariant Feature Extraction." *Remote Sensing* 13 (19): 3990. https://doi.org/10.3390/rs13193990.

Li, Pei, Zhao Dong, Xinyu Su, et al. 2024. "Application of High Adaptive Models in Building Damage Assessment: Case Studies of Earthquake in Turkey and Hurricane in Louisiana." *Journal of Applied Remote Sensing* 19 (1): 014501. https://doi.org/10.1117/1.JRS.19.014501.

Li, Yundong, Shi Ye, and Ivan Bartoli. 2018a. "Semisupervised Classification of Hurricane Damage from Postevent Aerial Imagery Using Deep Learning." *J. Appl. Rem. Sens.* 12 (04): 04. https://doi.org/10.1117/1.JRS.12.045008.

Li, Yundong, Shi Ye, and Ivan Bartoli. 2018b. "Semisupervised Classification of Hurricane Damage from Postevent Aerial Imagery Using Deep Learning." *Journal of Applied Remote Sensing* 12 (4): 045008. https://doi.org/10.1117/1.JRS.12.045008.

Liu, Chaoxian, Haigang Sui, and Lihong Huang. 2020a. "Identification of Building Damage from UAV-Based Photogrammetric Point Clouds Using Supervoxel Segmentation and Latent Dirichlet Allocation Model." *Sensors* 20 (22): 22. https://doi.org/10.3390/s20226499.

Liu, Chaoxian, Haigang Sui, and Lihong Huang. 2020b. "Identification of Building Damage from UAV-Based Photogrammetric Point Clouds Using Supervoxel Segmentation and Latent Dirichlet Allocation Model." *Sensors* 20 (22): 6499. https://doi.org/10.3390/s20226499.

Loizzo, R., R. Guarini, F. Longo, et al. 2018. “Prisma: The Italian Hyperspectral Mission.” *IGARSS 2018 - 2018 IEEE International Geoscience and Remote Sensing Symposium*, July, 175–78. https://doi.org/10.1109/IGARSS.2018.8518512.

Lubin, A., and A. Saleem. 2019. “Remote Sensing-Based Mapping of the Destruction to Aleppo during the Syrian Civil War between 2011 and 2017.” *Applied Geography* 108 (July): 30–38. https://doi.org/10.1016/j.apgeog.2019.05.004.

Marr, D., and Ellen Hildreth. 1980. “Theory of Edge Detection.” *Proceedings of the Royal Society of London. Series B, Containing Papers of a Biological Character. Royal Society (Great Britain)* 207 (February): 187–217. https://doi.org/10.1098/rspb.1980.0020.

Maxar. 2019. “In the Blink of an Eye – Looking Back on Nine Years with Tomnod.” Maxar Blog, August 1. https://blog.maxar.com/leading-the-industry/2019/in-the-blink-of-an-eye-looking-back-on-nine-years-with-tomnod.

McFeeters, S. K. 1996. “The Use of the Normalized Difference Water Index (NDWI) in the Delineation of Open Water Features.” *International Journal of Remote Sensing* 17 (7): 1425–32. https://doi.org/10.1080/01431169608948714.

Meyer, Franz. 2019. “Spaceborne Synthetic Aperture Radar: Principles, Data Access, and Basic Processing Techniques.” *Synthetic Aperture Radar (SAR) Handbook: Comprehensive Methodologies for Forest Monitoring and Biomass Estimation*, 21–64.

Mirza, Mehdi, and Simon Osindero. 2014. “Conditional Generative Adversarial Nets.” arXiv:1411.1784. Preprint, arXiv, November 6. https://doi.org/10.48550/arXiv.1411.1784.

Mueller, Hannes, Andre Groeger, Jonathan Hersh, Andrea Matranga, and Joan Serrat. 2021. “Monitoring War Destruction from Space Using Machine Learning.” *Proceedings of the National Academy of Sciences* 118 (23): e2025400118. https://doi.org/10.1073/pnas.2025400118.

Naeini, Mahdi Pakdaman, Gregory Cooper, and Milos Hauskrecht. 2015. “Obtaining Well Calibrated Probabilities Using Bayesian Binning.” *Proceedings of the AAAI Conference on Artificial Intelligence* 29 (1). https://doi.org/10.1609/aaai.v29i1.9602.

Neto, Antônio, and Daniel Dantas. 2024. “Building Damage Segmentation After Natural Disasters in Satellite Imagery with Mathematical Morphology and Convolutional Neural Networks:” *Proceedings of the 26th International Conference on Enterprise Information Systems*, 828–36. https://doi.org/10.5220/0012706300003690.

Novikov, German, Alexey Trekin, Georgy Potapov, Vladimir Ignatiev, and Evgeny Burnaev. 2018. “Satellite Imagery Analysis for Operational Damage Assessment in Emergency Situations.” In *Business Information Systems*, edited by Witold Abramowicz and Adrian Paschke. Springer International Publishing. https://doi.org/10.1007/978-3-319-93931-5_25.

O’Connor, Jack. 2024. *A Short Introduction to Geospatial Intelligence*. First edition. CRC Press, Taylor & Francis Group.

Oktay, Ozan, Jo Schlemper, Loic Le Folgoc, et al. 2018. “Attention U-Net: Learning Where to Look for the Pancreas.” arXiv:1804.03999. Preprint, arXiv, May 20. https://doi.org/10.48550/arXiv.1804.03999.

“Open Data Program.” n.d. Accessed August 30, 2025. https://www.maxar.com/open-data.

Plank, Simon. 2014. “Rapid Damage Assessment by Means of Multi-Temporal SAR — A Comprehensive Review and Outlook to Sentinel-1.” *Remote Sensing* 6 (6): 4870–906. https://doi.org/10.3390/rs6064870.

“Pléiades Neo Full Archive and Tasking - Earth Online.” n.d. Accessed August 30, 2025. https://earth.esa.int/eogateway/catalog/pleiades-neo-full-archive-and-tasking.

Pondi, Brian, Marius Appel, and Edzer Pebesma. 2024. “OpenEOcubes: An Open-Source and Lightweight R-Based RESTful Web Service for Analyzing Earth Observation Data Cubes.” *Earth Science Informatics* 17 (2): 1809–18. https://doi.org/10.1007/s12145-024-01249-y.

Presa-Reyes, Maria, and Shu-Ching Chen. 2020. “Assessing Building Damage by Learning the Deep Feature Correspondence of Before and After Aerial Images.” *2020 IEEE Conference on Multimedia Information Processing and Retrieval (MIPR)*, August, 43–48. https://doi.org/10.1109/MIPR49039.2020.00017.

Qing, Yuanzhao, Dongping Ming, Qi Wen, et al. 2022. “Operational Earthquake-Induced Building Damage Assessment Using CNN-Based Direct Remote Sensing Change Detection on Superpixel Level.” *International Journal of Applied Earth Observation and Geoinformation* 112 (August): 102899. https://doi.org/10.1016/j.jag.2022.102899.

Quinlan, J. R. 1986. “Induction of Decision Trees.” *Machine Learning* 1 (1): 81–106. https://doi.org/10.1007/BF00116251.

Rao, Anirudh, Jungkyo Jung, Vitor Silva, Giuseppe Molinario, and Sang-Ho Yun. 2023. *Earthquake Building Damage Detection Based on Synthetic-Aperture-Radar Imagery and Machine Learning*. 23 (2): 789–807. https://doi.org/10.5194/nhess-23-789-2023.

“Rapid Access Program | Commercial Imaging Satellites.” n.d. Accessed August 30, 2025. https://www.maxar.com/maxar-intelligence/products/rapid-access-program.

Rashidian, Vahid, Laurie Baise, Magaly Koch, and Babak Moaveni. 2021. “Detecting Demolished Buildings after a Natural Hazard Using High Resolution RGB Satellite Imagery and Modified U-Net Convolutional Neural Networks.” *Remote Sensing* 13 (11): 2176. https://doi.org/10.3390/rs13112176.

Richards, John A. 2022. *Remote Sensing Digital Image Analysis*. Springer International Publishing. https://doi.org/10.1007/978-3-030-82327-6.

Ronneberger, Olaf, Philipp Fischer, and Thomas Brox. 2015. “U-Net: Convolutional Networks for Biomedical Image Segmentation.” In *Medical Image Computing and Computer-Assisted Intervention – MICCAI 2015*, edited by Nassir Navab, Joachim Hornegger, William M. Wells, and Alejandro F. Frangi. Springer International Publishing. https://doi.org/10.1007/978-3-319-24574-4_28.

Scher, Corey, and Jamon Van Den Hoek. 2023. “Nationwide Mapping of Damage to Human Settlements across Ukraine Using Sentinel-1 InSAR Coherence Change Detection.” 2023 (December): GC23A-01. https://ui.adsabs.harvard.edu/abs/2023AGUFMGC23A..01S.

Scher, Corey, and Jamon Van Den Hoek. 2025. “Nationwide Conflict Damage Mapping with Interferometric Synthetic Aperture Radar: A Study of the 2022 Russia–Ukraine Conflict.” *Science of Remote Sensing* 11 (June): 100217. https://doi.org/10.1016/j.srs.2025.100217.

Selvakumaran, Sivasakthy, Iain Rolland, Luke Cullen, et al. 2025. “Improving Operational Use of Post-Disaster Damage Assessment for Urban Search and Rescue by Integrated Graph-Based Multimodal Remote Sensing Data Analysis.” *Progress in Disaster Science* 25 (January): 100404. https://doi.org/10.1016/j.pdisas.2025.100404.

Shelestov, Andrii, Sophia Drozd, Polina Mikava, Illia Barabash, and Hanna Yailymova. 2023. “War Damage Detection Based on Satellite Data.” Universitäts- und Landesbibliothek Sachsen-Anhalt, March. https://doi.org/10.25673/101924.

Shen, Yu, Sijie Zhu, Taojiannan Yang, et al. 2022. “BDANet: Multiscale Convolutional Neural Network With Cross-Directional Attention for Building Damage Assessment From Satellite Images.” *IEEE Trans. Geosci. Remote Sensing* 60: 1–14. https://doi.org/10.1109/TGRS.2021.3080580.

Shimada, Masanobu, Takuya Itoh, Takeshi Motooka, Manabu Watanabe, and Rajesh Thapa. 2016. "Generation of the First PALSAR-2 Global Mosaic 2014/2015 and Change Detection between 2007 and 2015 Using the PALSAR and PALSAR-2." *2016 IEEE International Geoscience and Remote Sensing Symposium (IGARSS)*, July, 3871–72. https://doi.org/10.1109/IGARSS.2016.7730004.

"SkySat Full Archive and New Tasking - Earth Online." n.d. Accessed August 30, 2025. https://earth.esa.int/eogateway/catalog/skysat-full-archive-and-new-tasking.

Small, David. 2011. "Flattening Gamma: Radiometric Terrain Correction for SAR Imagery." *IEEE Transactions on Geoscience and Remote Sensing* 49 (8): 3081–93. https://doi.org/10.1109/TGRS.2011.2120616.

Sokolova, Marina, and Guy Lapalme. 2009. "A Systematic Analysis of Performance Measures for Classification Tasks." *Information Processing & Management* 45 (4): 427–37. https://doi.org/10.1016/j.ipm.2009.03.002.

Soulakellis, Nikolaos, Georgios Tataris, Ermioni-Eirini Papadopoulou, et al. 2019. "Synergistic Exploitation of Geoinformation Methods for Post-Earthquake 3D Mapping and Damage Assessment." In *Intelligent Systems for Crisis Management*, edited by Orhan Altan, Madhu Chandra, Filiz Sunar, and Tullio Joseph Tanzi. Springer International Publishing. https://doi.org/10.1007/978-3-030-05330-7_1.

Su, Jinhua, Yanbing Bai, Xingrui Wang, et al. 2020. "Technical Solution Discussion for Key Challenges of Operational Convolutional Neural Network-Based Building-Damage Assessment from Satellite Imagery: Perspective from Benchmark xBD Dataset." *Remote Sensing* 12 (22): 3808. https://doi.org/10.3390/rs12223808.

"Swisstopo Fliegt Rapid-Mapping-Einsatz Bei Blatten." 2025. https://www.swisstopo.admin.ch/de/swisstopo-fliegt-rapid-mapping-einsatz-bei-blatten-20250520.

Taiwo H. Agbaje, Nemi Abomaye-Nimenibo, Chinedu James Ezeh, Abdullahi Bello, and Ayoola Olorunnishola. 2024. "Building Damage Assessment in Aftermath of Disaster Events by Leveraging Geoai (Geospatial Artificial Intelligence): Review." *World J. Adv. Res. Rev.* 23 (1): 1. https://doi.org/10.30574/wjarr.2024.23.1.2000.

Tan, Mingxing, and Quoc Le. 2019. "EfficientNet: Rethinking Model Scaling for Convolutional Neural Networks." *Proceedings of the 36th International Conference on Machine Learning*, May 24, 6105–14. https://proceedings.mlr.press/v97/tan19a.html.

Tang, Yizhuo, Zhengtao Cao, Ningbo Guo, and Mingyong Jiang. 2024. "A Siamese Swin-Unet for Image Change Detection." *Scientific Reports* 14 (1): 4577. https://doi.org/10.1038/s41598-024-54096-8.

Thenkabail, Prasad Srinivasa, John G. Lyon, and Alfredo Huete, eds. 2023. *Hyperspectral Remote Sensing of Vegetation*. Second edition. CRC Press.

Tilon, Sofia, Francesco Nex, Norman Kerle, and George Vosselman. 2020. "Post-Disaster Building Damage Detection from Earth Observation Imagery Using Unsupervised and Transferable Anomaly Detecting Generative Adversarial Networks." *Remote Sensing* 12 (24): 4193. https://doi.org/10.3390/rs12244193.

Torres, Ramon, Paul Snoeij, Dirk Geudtner, et al. 2012. "GMES Sentinel-1 Mission." *Remote Sensing of Environment*, The Sentinel Missions - New Opportunities for Science, vol. 120 (May): 9–24. https://doi.org/10.1016/j.rse.2011.05.028.

Touzani, Samir, and Jessica Granderson. 2021. "Open Data and Deep Semantic Segmentation for Automated Extraction of Building Footprints." *Remote Sensing* 13 (13): 2578. https://doi.org/10.3390/rs13132578.

"Ukraine Conflict Monitor ACLED." 2025. July 30. https://acleddata.com/monitor/ukraine-conflict-monitor.

"UN." 2025. https://www.un.org/en/.

"Unlocking The Power Of Space For Disaster Mitigation And Humanitarian…." n.d. Accessed August 30, 2025. https://blog.maxar.com/for-a-better-world/2025/unlocking-the-power-of-space-for-disaster-mitigation-and-humanitarian-action.

"UNOSAT." 2022. https://unosat.org/products/3300.

"UNOSAT." n.d. Accessed July 31, 2025. https://unosat.org/products/3371.

Van Zyl, Jakob, and Yunjin Kim. 2011. *Synthetic Aperture Radar Polarimetry*. JPL Space Science and Technology Series. Wiley. https://doi.org/10.1002/9781118116104.

Voigt, Stefan, Fabio Giulio-Tonolo, Josh Lyons, et al. 2016. "Global Trends in Satellite-Based Emergency Mapping." *Science* 353 (6296): 247–52. https://doi.org/10.1126/science.aad8728.

Voigt, Stefan, Thomas Kemper, Torsten Riedlinger, Ralph Kiefl, Klaas Scholte, and Harald Mehl. 2007. "Satellite Image Analysis for Disaster and Crisis-Management Support." *IEEE Transactions on Geoscience and Remote Sensing* 45 (6): 1520–28. https://doi.org/10.1109/TGRS.2007.895830.

Voigt, Stefan, Tobias Schneiderhan, André Twele, Monika Gähler, Enrico Stein, and Harald Mehl. 2011. "Rapid Damage Assessment and Situation Mapping: Learning from the 2010 Haiti Earthquake." *Photogrammetric Engineering & Remote Sensing* 77 (9): 923–31. https://doi.org/10.14358/PERS.77.9.923.

Wang, Lei, Xin Xu, Yue Yu, et al. 2019. "SAR-to-Optical Image Translation Using Supervised Cycle-Consistent Adversarial Networks." *IEEE Access* 7: 129136–49. https://doi.org/10.1109/ACCESS.2019.2939649.

Wang, Lili, Jidong Wu, Youtian Yang, Rumei Tang, and Ru Ya. 2024. "Deep Learning Models for Hazard-Damaged Building Detection Using Remote Sensing Datasets: A Comprehensive Review." *IEEE Journal of Selected Topics in Applied Earth Observations and Remote Sensing* 17: 15301–18. https://doi.org/10.1109/JSTARS.2024.3449097.

Wang, Ying, Alvin Wei Ze Chew, and Limao Zhang. 2022. "Building Damage Detection from Satellite Images after Natural Disasters on Extremely Imbalanced Datasets." *Automation in Construction* 140 (August): 104328. https://doi.org/10.1016/j.autcon.2022.104328.

Woodhouse, Iain H. 2017. *Introduction to Microwave Remote Sensing*. CRC Press. https://doi.org/10.1201/9781315272573.

Wu, Chuyi, Feng Zhang, Junshi Xia, et al. 2021. "Building Damage Detection Using U-Net with Attention Mechanism from Pre- and Post-Disaster Remote Sensing Datasets." *Remote Sensing* 13 (5): 905. https://doi.org/10.3390/rs13050905.

Wulder, Michael A., Thomas R. Loveland, David P. Roy, et al. 2019. "Current Status of Landsat Program, Science, and Applications." *Remote Sensing of Environment* 225 (May): 127–47. https://doi.org/10.1016/j.rse.2019.02.015.

Xia, Haobin, Jianjun Wu, Jiaqi Yao, et al. 2023. "A Deep Learning Application for Building Damage Assessment Using Ultra-High-Resolution Remote Sensing Imagery in Turkey Earthquake." *International Journal of Disaster Risk Science* 14 (6): 947–62. https://doi.org/10.1007/s13753-023-00526-6.

Xie, Boyi, Jeri Xu, Jungkyo Jung, et al. 2020. "Machine Learning on Satellite Radar Images to Estimate Damages After Natural Disasters." *Proceedings of the 28th International Conference on Advances in Geographic Information Systems* (Seattle WA USA), November, 461–64. https://doi.org/10.1145/3397536.3422349.

Xie, Haofeng, Xiangyun Hu, Huiwei Jiang, and Jinming Zhang. 2022. "BSSNet: Building Subclass Segmentation from Satellite Images Using Boundary Guidance and Contrastive Learning." *IEEE Journal of Selected Topics in Applied Earth Observations and Remote Sensing* 15: 7700–7711. https://doi.org/10.1109/JSTARS.2022.3202524.

Xie, Yakun, Dejun Feng, Hongyu Chen, et al. 2022. "Damaged Building Detection From Post-Earthquake Remote Sensing Imagery Considering Heterogeneity Characteristics." *IEEE Transactions on Geoscience and Remote Sensing* 60: 1–17. https://doi.org/10.1109/TGRS.2022.3200872.

Yuan, X., S. M. Azimi, C. Henry, et al. 2021. "AUTOMATED BUILDING SEGMENTATION AND DAMAGE ASSESSMENT FROM SATELLITE IMAGES FOR DISASTER RELIEF." *Int. Arch. Photogramm. Remote Sens. Spatial Inf. Sci.* XLIII-B3-2021 (June): 741–48. https://doi.org/10.5194/isprs-archives-XLIII-B3-2021-741-2021.

Yun, Sang-Ho, Kenneth Hudnut, Susan Owen, et al. 2015. "Rapid Damage Mapping for the 2015 Mw 7.8 Gorkha Earthquake Using Synthetic Aperture Radar Data from COSMO–SkyMed and ALOS-2 Satellites." *Seismological Research Letters* 86 (6): 1549–56. https://doi.org/10.1785/0220150152.

Zhang, Chenwei, Wenran Lu, Jiang Wu, Chunhe Ni, and Hongbo Wang. 2024. "SegNet Network Architecture for Deep Learning Image Segmentation and Its Integrated Applications and Prospects." *Academic Journal of Science and Technology* 9 (2): 224–29. https://doi.org/10.54097/rfa5x119.

Zhao, Fei, and Chengcui Zhang. 2020. "Building Damage Evaluation from Satellite Imagery Using Deep Learning." *2020 IEEE 21st International Conference on Information Reuse and Integration for Data Science (IRI)* (Las Vegas, NV, USA), August, 82–89. https://doi.org/10.1109/IRI49571.2020.00020.

ZHAO Jinling, HUANG Jian. 2024. "BDANet-Based Assessment of Building Damage from Earthquake Disasters." *Remote Sensing for Natural Resources* 36 (4): 193–200. https://doi.org/10.6046/zrzyyg.2023164.

Zhao, Zongze, Fenglei Wang, Shiyu Chen, Hongtao Wang, and Gang Cheng. 2024. "Deep Object Segmentation and Classification Networks for Building Damage Detection Using the xBD Dataset." *International Journal of Digital Earth* 17 (1): 1. https://doi.org/10.1080/17538947.2024.2302577.

Zheng, Zhuo, Yanfei Zhong, Junjue Wang, Ailong Ma, and Liangpei Zhang. 2021. "Building Damage Assessment for Rapid Disaster Response with a Deep Object-Based Semantic Change Detection Framework: From Natural Disasters to Man-Made Disasters." *Remote Sensing of Environment* 265: 112636. https://doi.org/10.1016/j.rse.2021.112636.

Zheng, Zhuo, Yanfei Zhong, Liangpei Zhang, Marshall Burke, David B. Lobell, and Stefano Ermon. 2024. "Towards Transferable Building Damage Assessment via Unsupervised Single-Temporal Change Adaptation." *Remote Sensing of Environment* 315 (December): 114416. https://doi.org/10.1016/j.rse.2024.114416.

Zhou, Zhi-Hua. 2012. *Ensemble Methods: Foundations and Algorithms*. 1st ed. Chapman & Hall/CRC.

Zhou, Zongwei, Md Mahfuzur Rahman Siddiquee, Nima Tajbakhsh, and Jianming Liang. 2018. "UNet++: A Nested U-Net Architecture for Medical Image Segmentation." Version 1. Preprint, arXiv. https://doi.org/10.48550/ARXIV.1807.10165.

Zhu, Jun-Yan, Taesung Park, Phillip Isola, and Alexei A. Efros. 2017. "Unpaired Image-to-Image Translation Using Cycle-Consistent Adversarial Networks." *2017 IEEE International*

Conference on Computer Vision (ICCV), October, 2242–51. https://doi.org/10.1109/ICCV.2017.244.

Zhu, Xiao Xiang, Devis Tuia, Lichao Mou, et al. 2017. "Deep Learning in Remote Sensing: A Comprehensive Review and List of Resources." *IEEE Geoscience and Remote Sensing Magazine* 5 (4): 8–36. https://doi.org/10.1109/MGRS.2017.2762307.

Ziemke, Jen. 2012. "Crisis Mapping: The Construction of a New Interdisciplinary Field?" *Journal of Map & Geography Libraries* 8 (2): 101–17. https://doi.org/10.1080/15420353.2012.662471.

Zitzlsberger, Georg, Michal Podhorányi, Václav Svatoň, Milan Lazecký, and Jan Martinovič. 2021. "Neural Network-Based Urban Change Monitoring with Deep-Temporal Multispectral and SAR Remote Sensing Data." *Remote Sensing* 13 (15): 3000. https://doi.org/10.3390/rs13153000.

2.8 Disclaimer

The preparation of this thesis involved a structured workflow combining extensive manual reading, systematic literature management, and selective use of AI-based tools to support

efficiency and consistency. The primary foundation of the work rests on the author's direct engagement with the scientific literature, critical assessment of sources, and manual drafting of summaries and arguments. Artificial intelligence was employed as an auxiliary tool, never as a replacement for scholarly judgment.

Approximately 165 scientific papers relevant to the topic of battlefield damage assessment of urban structures were initially identified via Google Scholar searches. These publications were imported into Zotero, where each entry was supplemented with a full-text PDF and an associated structured note. Notes followed a standardized template including metadata, extracted data fields (keywords, models, datasets, satellites, methods), and a layered summary (context, methodology, results, conclusions). Each referenced paper was read and evaluated by the author; summaries were drafted manually, supported where appropriate by Adobe AI-generated abstracts, which were always verified and corrected against the original texts.

Markdown notes were processed through a custom Python pipeline that normalized metadata, extracted datasets and satellites, created keywords, and ensured interoperability with Obsidian for relational graph visualization. AI support was used here primarily Regex in the Python pipeline. For technical tasks such as metadata normalization, DOI resolution, and error checking of bibliographic entries Python scripts were used. For the identification of highly cited primary works, ChatGPT 4.0/5 (Version of July / August 2025) was employed in conjunction with relational graph analyses; candidate references were cross-verified manually via Google Scholar citation counts before inclusion.

Draft chapters of the appendices and literature overview were written manually, based on the structured notes and critical reading. ChatGPT was subsequently used in an editorial capacity to propose rephrasings, ensure consistency in academic style, and generate alternative formulations. The AI-generated text was not adopted verbatim; instead, it was carefully fact-checked, compared with the cited sources, and revised by the author. Similarly, scite.ai was used as a supplementary tool to verify the context of citations within the scientific discourse. All final references were inserted manually via Zotero to ensure accuracy and compliance with citation standards.

This integrated workflow allowed for efficient processing of a large body of literature while ensuring academic integrity. The critical reading, interpretation, selection of relevant findings, structuring of arguments, and final phrasing of all content were conducted by the author. AI tools contributed to metadata processing, drafting of preliminary summaries, language refinement, and bibliometric checks, but the responsibility for accuracy, interpretation, and argumentation rests fully with the author.